EXPERIMENTAL AND NUMERICAL STUDY ON VIBRATION AND BUCKLING CHARACTERISTICS OF LAMINATED COMPOSITE PLATES

A thesis submitted in partial fulfillment of the requirements for the degree of

Bachelor of Technology
In
Civil Engineering

By
Samikshya Meher
(109CE0046)

Nishant Nayak
(109CE0054)

Under The Guidance of

Prof. Shishir Kumar Sahu

Department of Civil Engineering
National Institute of Technology Rourkela
Orissa -769008, India

May 2013

DEPARTMENT OF CIVIL ENGINEERING
NATIONAL INSTITUTE OF TECHNOLOGY
ROURKELA, ODISHA-769008

CERTIFICATE

This is to certify that the thesis entitled, **"EXPERIMENTAL AND NUMERICAL STUDY ON VIBRATION AND BUCKLING CHARACTERISTICS OF LAMINATED COMPOSITE PLATES"** submitted by **SAMIKSHYA MEHER** bearing roll no. **109CE0046** and **NISHANT NAYAK** bearing roll no. **109CE0054** of C**ivil Engineering Department,** National Institute of Technology, Rourkela is an authentic work carried out by them under my supervision and guidance.

To the best of my knowledge, the matter embodied in the thesis has not been submitted to any other University / Institute for the award of any Degree or Diploma.

Date: 10th May, 2013
Place: Rourkela

Prof. Shishir Kr. Sahu
Department of Civil Engineering
National Institute of Technology
Rourkela, Odisha-769008

ACKNOWLEDGEMENTS

We would like to express our deep sense of gratitude to our supervisor **Prof. Shishir Kumar Sahu** for giving us this opportunity to work under him. Each and every discussion with him has been very educative. We are very thankful to him for the patience he had with us and for giving us absolute freedom in doing our task. We shall remain indebted to him for his constant support and guidance.

We are thankful to **Prof. N. Roy**, Head of the department, Department of Civil Engineering for providing us with necessary facilities for the research work.

We extend our heartfelt gratitude to **Prof. Pradip Sarkar** and **Prof. A.V. Asha** for the timely help without which this work would not have been successful.

We are grateful to Structural Engineering Laboratories for providing us with full laboratory facilities. We express our thanks to all the laboratory staff, especially Mr. Ramanus Lugun for his constant help and support at the time of need.

One other contribution which cannot be passed unacknowledged is the FRP Composites Lab and INSTRON Lab, Department of Metallurgy and Material Sciences and Production Engineering Lab, Department of Mechanical Engineering. We are really thankful to **Mr. Dinesh Kumar Rathore**, **Mr. Himanshu Sekhar Panda**, **Mrs. Sanghamitra Sethi** and **Mr. Kanhu Charan Nayak** for their ever ready help and cooperation.

A truly unbounded words of thanks our family for their affection, constant encouragement and forbearance. Thanks to the Almighty for the blessing that he has bestowed upon us in all our endeavors.

Samikshya Meher
109CE0046
Department of Civil Engineering
National Institute of Technology
Rourkela

Nishant Nayak
109CE0054
Department of Civil Engineering
National Institute of Technology
Rourkela

ABSTRACT

Composite materials are being increasingly used in automotive, civil, marine, and especially weight sensitive aerospace application, primarily because of its specific strength and stiffness. This necessitates studies on vibration and buckling behaviour of the structures. Most of the analysis on vibration of composite plates is done either analytically or by different numerical methods. Very little is reported on the experimental investigation of laminated composite plates using the present state of the art instrumentation or measurement. The present research is mostly experimental study based on vibration measurement and buckling behaviour of industry driven woven fiber composite panels for different layer thickness. The effects of different geometry, boundary conditions, aspect ratio and type of fiber on the natural frequencies of vibration of woven fiber composite panels are studied in this investigation. The effects of variation in temperature and moisture concentration due to hygrothermal conditioning, on the natural frequencies are also investigated. Critical buckling load is determined for laminates with various thicknesses. Experiments have also been conducted to study the vibration and buckling characteristics of carbon/glass hybrid plates for different lamination sequence and percentage of carbon and glass fiber. A finite element package, ANSYS 13.0 was used to obtain the numerical results and plot the mode shapes for various modes of vibration.

The composite plates of different layers are manufactured using woven carbon fiber by hand lay-up method followed by cutting to required dimension. The free vibration characteristics are studied with First Fourier Transform (FFT) analyzer, accelerometer using impact hammer excitation. The Frequency Response Function (FRF) is studied using Pulse Lab Shop to obtain a clear understanding of the vibration characteristics of the specimen. The critical buckling load is determined using INSTRON 1195.

From the results obtained it was observed that, the frequencies of vibration as well as critical buckling load increased with increase in thickness. For different boundary conditions, the modal frequencies were determined to be highest in case of fully clamped condition in comparison to all other boundary conditions. It was also observed that with increasing aspect ratio there is a gradual increase in the modal frequencies obtained, due to higher stiffness. As the conditioning temperature deviates from the manufacturing temperature, the natural frequencies decrease gradually. The increase in moisture concentration of the laminate results in decrease in the modal frequencies. When compared to Glass fiber reinforced polymer

(GFRP) the natural frequencies of vibration obtained from Carbon fiber reinforced polymer (CFRP) plates were found to be significantly higher which is representative of their higher specific strength. The results of buckling tests showed that the buckling load increases with increase in thickness of the laminate.

The studies concluded that the samples when subjected to thermal conditioning for ample time lose their stiffness and so the modal frequencies decrease. The decrease in the frequencies is proportional to the temperature difference between the conditioning temperature and the manufacturing temperature. Absorption of moisture at temperatures well above room temperature also leads to damage of the laminate and so the modal frequencies decrease. The fatigue testing done by repeatedly exposing the sample to a particular temperature, attain a constant value of stiffness after reduction in initial few iterations.

The studies on hybrid plates show that they possess the advantages of both their constituent fibres and have properties intermediate to the properties of individual fibres. The effect of percentage composition and sequence of lamination of the fibres on vibrational and buckling characteristics of the composite plates were observed. It was observed that the failure due to tensile load in hybrids is governed by delamination between layers. The values of vibrational analysis present similar conclusions with regards to stiffness of plates as obtained from the tensile tests. The buckling results show that stiffer materials on outermost layer give maximum buckling strength compared to those with carbon fibres in inner layers.

TABLE OF CONTENTS

LIST OF FIGURES

LIST OF TABLES

CHAPTER -1

INTRODUCTION

1.1 Introduction

Composite materials have extensive applications in various fields including fuselage panels of aeroplane, turbine blades, automobile body panels, cryogenic fuel tanks etc. They have various architectural applications such as siding, cladding, roofing, flooring etc. Woven fabric composites are a class of textile composite materials with a fully integrated, continuous spatial fibre network that provide excellent integrity and conformability for advanced structural composite applications. These materials have gained tremendous popularity for possessing excellent durability, corrosion resistance and high strength to weight ratio. Anti-seismic behaviour, ease of installation, versatility, excellent fatigue behaviour, electromagnetic neutrality, and fire resistance make it a better alternative to steel and other alloys. Thus, the vibration characteristics of the woven fibre laminated composite panels are of tremendous practical importance in prediction of the dynamic behaviour of composite panels.

1.2 Importance of present study

Most of the investigations were focused either on numerical analysis of unidirectional composite plates or static or impact studies, damage initiation or failure mode of woven or braided composite plates. The computation of natural frequencies and buckling load is important to predict the behaviour of structures under dynamic loads. Modal analysis is used for prediction of dynamic properties of structures. The modal analysis can be used a non-destructive technique of assessment of stiffness of structures. Measurement of changes in vibrational characteristics can be used to detect, locate and roughly quantify damage in CRPF panels. The deviation of natural frequencies is an indication of the presence of invisible defect that cannot be determined otherwise. This study is also necessary in order to avoid resonance of large structures under dynamic loading. During designing of structures subjected to compressive loading, knowledge of buckling characteristics of the comprising elements is necessary in order to prevent overloading

of the structure.

1.3 Outline of the present work

The present study mainly deals with the vibration and buckling characteristics of laminated composite plates. The effects of number of layers, aspect ratio, boundary condition, hygrothermal treatment and type of fiber on vibrational behaviour of CFRP plates were examined. The influence of lamination sequence of glass-carbon/epoxy composite laminates on the free vibration and buckling behaviour was studied. Tests were conducted to experimentally determine the influence of the above parameters and the obtained results were validated using finite element package, ANSYS 13.0.

This thesis contains five chapters. The first chapter presents a brief introduction on the importance and application of the present study.

In Chapter 2, the literature review for the various studies conducted in the present study has been enlisted along with a critical discussion of investigations conducted. This chapter also includes the aim and scope of the present study.

In Chapter 3, the finite element formulation for the solution of vibration problem due to hygrothermal loading as well as buckling problem has been presented. A subsequent computer program has been developed in accordance with the formulation.

In Chapter 4, the procedure for modeling composite laminates using finite element package ANSYS 13.0, has been described stepwise.

In Chapter 5, the detailed experimental procedure for casting the specimen, determining the physical properties and hygrothermal conditioning has been described. The procedure for determination of modal frequencies of composite laminates subjected to various parametric changes, by using FFT analyzer has been mentioned along with the procedure for determination of buckling load of carbon and hybrid plates.

In Chapter 6, the results obtained from the present investigation have been presented and discussed in detail. The effects of various parameters such as number of layers, aspect ratio, boundary condition, temperature conditioning, moisture concentration and type of fibre on the free vibration of carbon fibre composite plates are presented. Finite element results obtained for the above parameters using ANSYS has also been included. Results on the buckling analysis of CFRP plates with varying thickness and hybrid plates with different lamination sequence have been explained in details.

In Chapter 7, the conclusion drawn on the above studies have been described with a brief description on the scope of further study on this area.

In Chapter 8, the future scope of the present study has been presented.

CHAPTER -2

REVIEW OF LITERATURE

2.1 Introduction

The computation of natural frequencies is important to predict the behaviour of structures under dynamic loads. The modal analysis can be used a non-destructive technique of assessment of stiffness of structures. Measurement of changes in vibrational characteristics can be used to detect, locate and roughly quantify damage in CRPF panels. This study is also necessary in order to avoid resonance of large structures under dynamic loading. Buckling analysis is required to check the dynamic stability of the various structural components of civil and aerospace structures under in plane loading. The related literature was critically reviewed so as to provide the background information on the problems to be considered in the research work and to emphasize the relevance of the present study. Most of them are limited to theoretical results by adopting various methods particularly with unidirectional fibres. The experimental results on vibration measurement or modal analysis of composite plates are less in open literature.

The literature reviewed for the above studies are grouped into the following

1. Vibration of laminated carbon composite plates
2. Buckling of laminated carbon composite plates
3. Glass-carbon/epoxy hybrid plates

2.2 Vibration of laminated carbon composite plates

Cawley and Adams (1978) investigated the natural modes of square aluminium plates and square composite plates with different ply orientations for free-free boundary conditions, both theoretically as well as experimentally. Cawley and Adams (1979) also used dynamic analysis to

detect, locate and roughly quantify damage to components fabricated from fibre reinforced plastic. Crawley (1979) experimentally determined the mode shapes and natural frequencies of composite plates, cylindrical shell sections and Aluminium hybrid plates for various laminates and aspect ratio using electro-magnetic shaker and compared the results to that obtained from finite element analysis. The natural frequency and the specific damping capacity of CFRP and GFRP were predicted by Lin *et al*. (1984) using zoom-FFT based on transient testing technique and computer based programme implementing finite element method. Chai (1994) presented an approximate method based on Rayleigh-Ritz approach to determine the free vibration frequencies of generally laminated composites for different ply orientation and different boundary conditions. Maiti and Sinha (1996) used the first order shear deformation theory and higher order shear deformation theories to develop FEM methods to study the bending, free vibration and impact response of thick laminated composite plates. The effects of delamination on the free vibration of composite plates were analysed by Ju *et al.* (1995). Chen and Chou (1998) developed 1D elasto-dynamic analysis method for vibration analysis orthogonal woven fabric composites. The free vibration frequencies of cross ply laminated square plates for twelve different boundary conditions were determined using Ritz method by Aydogdu and Timarci (2003). Ferreira *et al.* (2005) conducted analytical studies using FSDT in radial basis functions procedure for moderately thick symmetrically laminated composite plates. Xiang *et al.* (2009) carried out theoretical studies of laminated composite plates using Guassian radial basis functions and first order shear deformation theory. Xiang and Wang (2009) studied the free vibration analysis of symmetric laminated composite plates using trigonometric theory and inverse multiquadriatic radial basis function. Maheri (2010) used theoretical predictions of modal response of square layered FRP panel to study the variation of modal damping under various boundary conditions. Also the variation of modal damping with the fiber orientation of the two outermost layers of the panel with a view to possibly manipulation of this orientation in order to maximize the modal analysis is studied.

However vibration of industry driven woven fiber composite plates are scarce in literature. Linear analysis on CFRP faced sandwich plates with an orthotropic aluminium honeycomb core has done using principle of minimum total potential and double Fourier series by Kanematsu *et al*. (1988). Chai *et al.* (1993) used TV holography technique to obtain the vibrational response of the unidirectional laminated carbon fibre-epoxy plates and carried out finite element studies

simultaneously. Chakraborty *et al.* (2000) determined the frequency response of GFRP plates experimentally and validated the results using commercial finite element package (NISA). The analytical values were compared with the experimental values obtained with fully clamped boundary condition. Holographic technique was used to study the modes and deflection. Hwang and Chang (2000) used impulse technique for vibration testing of composite plates for determination elastic constants of materials and modelled undamped free vibration using ANSYS 5.3. Lei *et al.* (2010) studied the effect of different woven structures of the glass fibre on the dynamic properties of composite laminates.

The present study deals with modal testing of CRFP plates and compared with the numerical modelling using finite element in MATLAB environment and also by ANSYS. Various mode shapes are plotted using ANSYS and discussed. The effects of different geometry, boundary conditions and lamination parameters on the frequencies of vibration of carbon fiber reinforced polymer (CFRP) panels are studied in this investigation.

2.2.1 Vibration analysis of composite plates subjected to hygrothermal loading

The impact of environmental factors such as variation in temperature and humidity concentration on composite materials behavior are of significant concern for the aircraft industry since storage and operating conditions vary considerably and can add to the wear and tear of structural components. The studies conducted on prediction of dynamic behaviour of composite laminates were mostly based on analytical and finite element method.

Whitney and Ashton (1975) considered the effect of environment on the free vibration of symmetric and unsymmetric laminated plates, using the Ritz method based upon the classical laminated plate theory. Collings and Stone (1985) conducted theoretical analysis of strains induced due to variation in temperature and moisture concentration in CFRP and experimentally determined the magnitude of strain and coefficients of moisture expansion. Chang and Jen (1986) analysed the nonlinear free vibration of a heated orthotropic rectangular thin plate under various boundary condition using Von Karman's nonlinear plate theory and Berger's nonlinear plate analysis method. Dhanaraj and Palaninathan (1989) presented results on effects of temperature on free vibrational characteristics of antisymmetric laminates. The effect of hygrothermal conditioning on vibrational frequencies of laminated composite plates was studied

analytically using finite element method by Sairam and Sinha (1992). Galea and White (1993) investigated the effects of temperature on the dynamic response of thin CFRP plates experimentally as well as analytically using finite element method. Eslami and Maerz (1995) studied the effect of unsteady temperature and moisture environment on free vibration of symmetric cross-ply laminated plates. Parhi *et al.* (2000) analytically studied the effects of curvature and lamination scheme with varying hygrothermal conditions on variation of fundamental frequency of single and multiple delaminated plates and shells. Choi *et al.* (2001) examined the effects of matrix volume ratio, void volume ratio, specimen thickness, lay-up sequence and applied bending load on various hygroscopic aspects of composite laminates. Patel *et al.* (2002) studied the effect of moisture and temperature on the linear free vibration of laminated composite plates using first order and higher order shear deformation theories. Huang *et al.* (2004) used higher order shear deformation plate theory based on micromechanical model to explain the effect of temperature and moisture on the non-linear vibration and dynamic response of shear deformable laminates. Botelho *et al.* (2005) presented the influence of hygrothermal conditioning on the natural frequencies of glass/epoxy, aluminum and Glare laminates. Lo *et al.* (2010) analysed the response of laminated composite plates to temperature and moisture concentration variation by incorporating refined higher order theory and discrete Kirchoff quadrilateral thin plate element. Panda *et al.* (2013) conducted numerical as well as experimental studies on vibration characteristics of delaminated composite plates under hygrothermal conditioning. In this study they presented the effects of temperature, moisture, delamination size and boundary conditions on the modal frequencies of woven fibre Glass/Epoxy composite plates.

From the reviewed literature it was observed that experimental studies on hygrothermal effects on vibration characteristics of carbon composite panels are scare in open source literature. The available studies mostly revolved around glass fibre composites. In the present study, the behaviour of carbon fibre composite plates are studied using experimental techniques and the obtained results were validated using finite element method.

2.3 Buckling of laminated carbon composite plates

First order shear deformation theory along with various strain displacement relationships has been used Singh *et al.* (1989), Sundaresan *et al.* (1996) and Zhong and Gu (2007) to develop

FEM models to study the effects of different parameters on the critical buckling load. Buckling analysis was performed by BENST module of the PLANS system of finite element structural analysis programs by Pascal (1978) for simply supported plates with laminate material properties varying from mildly orthotropic to severely orthotropic. Leissa (1983) conducted an extensive study on buckling of composite plates including classical bifurcation buckling analysis and complicating effects. She examined buckling of composite plates and provided increased perspective and organization to a very complicated subject. Lagace *et al.* (1986) conducted an experimental and analytical investigation to study the effect of mechanical coupling on anisotropic plate. Rayleigh Ritz energy analysis is used to determine the mode shapes and classical buckling loads of various laminates analytically. Palardy and Palazotto (1990) studied buckling and vibration characteristics of laminated cross ply using the Levy approach. The plate model includes effects of shear deformation and rotary inertia. The effects of transverse shear on stability of laminated composite plates under uniaxial and biaxial compression were studied by Singh and Rao (1989) for different boundary conditions. They developed an eight noded, shear flexible quadratic rectangular element with five degrees of freedom per node. FEM based technique based on shear deformable plate model has been used by Bruno and Lato (1991) to study the buckling behaviour of anisotropic plates. Chai and Hun (1992) used total potential energy approach in conjugation with Rayleigh Ritz approach. Kam and Chang (1992) performed the buckling analysis of laminated composite plates by developing a shear deformable finite element. Optimal lamination arrangements of layers were determined for maximizing buckling load of plates. Chai and Khong (1993) used a semi-numerical approach to study the effect of support conditions. Aiello and Ombres (1997) also used first order shear deformation theory and Rayleigh Ritz method to determine the critical buckling load of flat hybrid laminates under in-plane loading and shear forces for simply supported boundary conditions. The advantages of hybridization over non-hybrid laminates have been assessed. Mania (2005) presented the results of buckling analysis of layered isosceles trapezoidal plate subjected to in-plane compression under simply supported boundary condition. The influence of size of plates and bending stiffness on critical load parameter for clamped orthotropic plate under shear was analyzed by Lopatin and Korbut (2006). Topal and Uzman (2007) performed optimization to maximize the buckling load capacity of laminated plates subjected to in-plane static loads for simply supported boundary condition. They also studied the effect of width to thickness ratio, aspect ratio, number of layers,

material anisotropy, load ratio and uncertainties in material properties. Panda and Ramachandra (2010) presented analytical results for nine different sets of boundary conditions under non uniform loading and compared the obtained results with that of ANSYS. Dash and Singh (2012) used higher order shear deformation theory with Green Lagrange non-linear strain displacement relationships for studying the buckling and post-buckling characteristics of laminated composite plates. Seifi *et al*. (2012) performed studies on critical buckling load under uniform internal and external radial edge loads of annular plates using energy method. Ovesy *et al*. (2013) presented buckling analysis of moderately thick symmetric cross plies laminated plates and plate structure using an exact finite strip.

In this investigation, the effect of number of plies on the critical buckling load of carbon/epoxy composite panels have been studied experimentally as well as using finite element method.

2.4 Glass-Carbon/epoxy hybrid composite plates

Bunsell and Harris (1974) studied the properties and failure characteristics of glass/carbon hybrid laminates and suggested that light and economical engineering materials with required properties can be prepared by mixing two different fibres. Ni *et al*. (1984) developed mathematical formulation using energy method finite element analysis to predict the dynamic characteristics of hybrid laminated composite beams and plates respectively. The obtained results were compared with experimental results. They also studied the economic aspects and considerations of using hybrid materials over usual composite laminates with only one type of fibre. Iyengar and Umeritiya (1986) used Galerkin method to numerically compute the free vibration response of hybrid, laminated rectangular and skewed plates for different aspect ratio and fiber angle. They showed that with increase in aspect ratio the frequency decreases, for a given skew angle and the rigidity of the skew plate increases with an increase in skew angle. Iyengar and Umeritiya (1986) performed analytical studies on the deflection of Kevlar/epoxy and boron/epoxy hybrid laminated plates by applying Galerkin technique and concluded that the hybrid laminates turn out to be lighter for a specific deflection. Barai and Durvasula (1992) studied the effects of curvature, aspect ratio, stacking sequence and ply orientation on the vibration and buckling characteristics of curved panels of hybrid laminates using Reissners's shallow shell theory and first order shear deformation theory. From the obtained results, they concluded that natural

frequencies are enhanced due to curvature and are more predominant for thinner panels. Naik *et al*. (2001) experimentally determined the impact response and post impact compressive characteristics glass-carbon/epoxy hybrid laminates with alternate stacking sequence by using instrumented drop weight impact test apparatus. They observed that the hybrid laminates were found to be fewer notches sensitive when compared to pure carbon or glass composites. Badie *et al*. (2011) computed the fatigue life of drive shafts using finite element analysis. They studied the effect of fibre orientation and stacking sequence in hybrid laminates both analytically and experimentally.

From the available literature it was observed that no experimental studies were reported on the vibration and buckling characteristics of industry driven woven fibre Carbon-glass/epoxy hybrid laminates. Most of the studies conducted were based on analytical methods. The experimental results to study the effect of lamination sequence on the vibration and buckling characteristics have been reported in the present study.

2.5 Objective and scope of present study

The objective of this research is to study experimentally the vibration and buckling characteristics of composite laminates. Studies are conducted on CFRP as well as glass-carbon/epoxy composite plates. The obtained results are compared with the theoretical values based on FEM. The present study can be split into three different modules as below.

1. Vibration of laminated carbon composite plates
2. Buckling of laminated carbon composite plates
3. Glass-carbon/epoxy hybrid plates

The effects of different parameters including number of layers, aspect ratio, support conditions and effect of fiber on the vibration characteristics of industry driven woven fibre carbon composite panels are investigated. The effects of hygrothermal conditions on the vibration behavior of composite plates are also studied. The mode shapes for different boundary conditions are to be obtained using finite element package, ANSYS 13.0. The variation in the buckling loads with change in the number of layers of carbon fibre is observed. The effect of lamination sequence and percentage composition of carbon fibre on natural frequencies and critical buckling load of glass-carbon/epoxy hybrid plates is also studied.

CHAPTER -3

MATHEMATICAL FORMULATION

3.1 Introduction

The vibration analysis is carried out using the finite element method (FEM) with first order shear deformation theory (FSDT), considering the effects of transverse shear deformation and rotary inertia. An eight-node isoparametric quadratic element is employed in the present analysis with five degrees of freedom per node. Element elastic stiffness matrices, mass matrices and load vectors are derived using the principle of Stationery Potential Energy. They are evaluated using the Gauss quadrature numerical integration technique. The overall stiffness and mass matrices are obtained by assembling the corresponding element matrices using skyline technique. Computer programs are developed by using FEM to determine natural frequencies and critical buckling load of woven fibre laminated composite plates.

3.2 Vibration of Plate with Hygrothermal Loading

The mathematical formulation for free vibration of laminated composite plates subjected to moisture and temperature are presented. Consider a laminated plate of uniform thickness 't' consisting of a number of thin lamiae, each of which may be arbitrarily oriented at an angle 'θ' with reference to the X-axis of the co-ordinate system as shown in Figures 1 and 2.

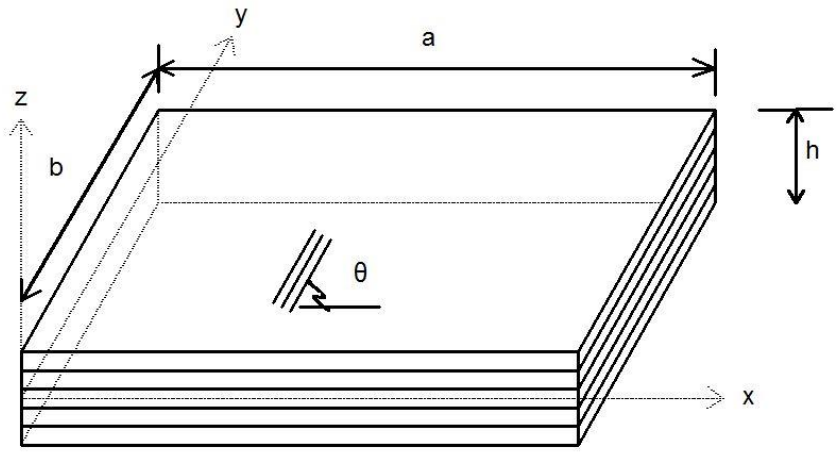

Figure 1 - Arbitrarily oriented laminated plate

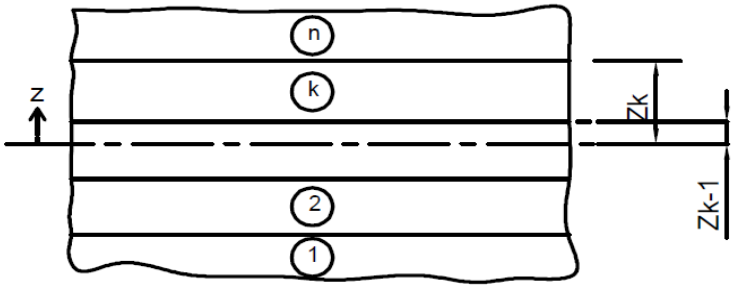

Figure 2 - Geometry of a n-layered laminate

3.2.1 Governing Equation for Vibration

The governing equations for the structural behavior of the laminated composite plates derived on the basis of first order shear deformation theory. The constitutive relations for the plate subjected to moisture and temperature given by:

$$\{F\} = [D]\{\varepsilon\} - \{F^N\} \qquad (1)$$

Where

$$\{F\} = \{N_x, N_y, N_{xy}, M_x, M_y, M_{xy}, Q_x, Q_y\}^T$$
$$\{F^N\} = \{N_x{}^N, N_y{}^N, N_{xy}, M_x{}^N, M_y{}^N, M_{xy}{}^N, 0, 0\}^T$$
$$\{\varepsilon\} = \{\varepsilon_x, \varepsilon_y, \gamma_{xy}, K_x, K_y, K_{xy}, \varphi_x, \varphi_y\}^T$$

$$[D]=\begin{bmatrix} A_{11} & A_{12} & A_{16} & B_{11} & B_{12} & B_{16} & 0 & 0 \\ A_{12} & A_{22} & A_{26} & B_{12} & B_{22} & B_{26} & 0 & 0 \\ A_{16} & A_{26} & A_{66} & B_{16} & B_{26} & B_{66} & 0 & 0 \\ B_{11} & B_{12} & B_{16} & D_{11} & D_{12} & D_{16} & 0 & 0 \\ B_{12} & B_{22} & B_{26} & D_{12} & D_{22} & D_{26} & 0 & 0 \\ B_{16} & B_{26} & B_{66} & D_{16} & D_{26} & D_{66} & 0 & 0 \\ 0 & 0 & 0 & 0 & 0 & 0 & S_{44} & S_{45} \\ 0 & 0 & 0 & 0 & 0 & 0 & S_{45} & S_{55} \end{bmatrix}$$

Where, N_x, N_y, N_{xy} = in-plane internal stress resultants.

M_x, M_y, M_{xy} = internal moment resultants.

Q_x, Q_y = transverse shear resultants.

$N_x{}^N, N_y{}^N, N_{xy}{}^N$ = in-plane non-mechanical stress resultants due to moisture and temperature.

$M_x{}^N, M_y{}^N, M_{xy}{}^N$ = non-mechanical moment resultants due to moisture and temperature.

$\varepsilon_x, \varepsilon_y, \gamma_{xy}$ = in-plane strains of the mid-plane.

K_x, K_Y, K_{xy} = Curvature of the plate

φ_x, ϕ_y = Shear rotations in x-z and y-z planes, respectively.

The non-mechanical force and moment resultants due to moisture and temperature are expressed as follows.

$$\left\{N_x{}^N, N_y{}^N, N_{xy}{}^N\right\}^T = \sum_{K=1}^{n}\left(\overline{Q_{ij}}\right)\{e\}_k\left(z_k - z_{k-1}\right) \qquad \text{For} \quad i, j = 1, 2, 6$$

$$\left\{M_x{}^N, M_y{}^N, M_{xy}{}^N\right\}^T = \frac{1}{2}\sum_{K=1}^{n}\left(\overline{Q_{ij}}\right)_k\{e\}_k\left(z_k{}^2 - z_{k-1}{}^2\right) \quad \text{For} \quad i, j = 1, 2, 6 \qquad (2)$$

Where

$$\{e\}_k = \{e_x, e_y, e_{xy}\}^T = [T]\{\beta_1\beta_2\}_k{}^T\left(C - C_O\right) + [T]\{\alpha_1\alpha_2\}_k{}^T\left(T - T_O\right), \text{ in which}$$

$[T]$ = Transformation matrix due to moisture and temperature and is given as

$$[T]=\begin{bmatrix} \cos^2\theta & \sin^2\theta \\ \sin^2\theta & \cos^2\theta \\ \sin 2\theta & \cos 2\theta \end{bmatrix}$$

e_x, e_y, e_{xy} = non-mechanical strains due to moisture and temperature

β_1, β_2 = moisture coefficient along 1 and 2 axes of lamina, respectively

$\alpha_1.\alpha_2$ = thermal coefficients along 1 and 2 axes of lamina, respectively

T, T_O =Elevated and reference moisture concentrations

$$\left(A_{ij}, B_{ij}, D_{ij}\right) = \sum_{k=1}^{n} \int_{z_{k-1}}^{k} \left[Q_{ij}\right]_k \left(1, z, z^2\right) \mathrm{dz} \qquad \text{(i, j =1.2.6)} \qquad (3)$$

$$S_{ij} = \kappa \sum_{k=1}^{n} \int_{z_{k-1}}^{k} \left[Q_{ij}\right]_k \, dz \qquad \text{(i, j =4,5)}$$

A_{ij}, B_{ij}, D_{ij} are the extensional, bending-stretching coupling and bending stiffness and κ is the shear correction factor.

$\left(\overline{Q_{ij}}\right)_{\mathrm{k}}$ in equations 11 and 12 is defined as:

$$[\overline{\mathrm{Q_{ij}}}]_k = [T_1]^{-1}\left[Q_{ij}\right]_k [T_1]^{-T} \qquad (i, j = 1, 2, 6) \qquad (4)$$

$$\left[\overline{Q}_{ij}\right]_k = [T_2]^{-1}\left[Q_{ij}\right]_k [T_2] \qquad (i, j = 4, 5)$$

Where $$[T_1] = \begin{bmatrix} \cos^2\theta & \sin^2\theta & \sin\theta\cos\theta \\ \sin^2\theta & \cos^2\theta & -\sin\theta\cos\theta \\ -2\sin\theta\cos\theta & 2\sin\theta\cos\theta & \cos^2\theta - \sin^2\theta \end{bmatrix}$$

$$[T_2] = \begin{bmatrix} \cos\theta & \sin\theta \\ -\sin\theta & \cos\theta \end{bmatrix}$$

$$\left[Q_{ij}\right]_k = \begin{bmatrix} Q_{11} & Q_{12} & 0 \\ Q_{12} & Q_{22} & 0 \\ 0 & 0 & Q_{66} \end{bmatrix} \qquad \text{For} \quad i, j = 1, 2, 6$$

$$\left[Q_{ij}\right]_k = \begin{bmatrix} Q_{44} & 0 \\ 0 & Q_{55} \end{bmatrix} \qquad \text{For} \quad i, j = 4, 5$$

In which

$$Q_{11} = \frac{E_{11}}{(1-\nu_{12}\nu_{21})}, Q_{12} = \frac{E_{11}\nu_{21}}{(1-\nu_{12}\nu_{21})}, Q_{21} = \frac{E_{22}\nu_{12}}{(1-\nu_{12}\nu_{21})}, Q_{22} = \frac{E_{22}}{(1-\nu_{12}\nu_{21})}, Q_{66} = G_{12}$$

E_{11}, E_{22} = Young's moduli of a lamina along and across the fibers, respectively

G_{12}, G_{13}, G_{23} = Shear moduli of a lamina with respect to 1, 2 and 3 axes

ν_{12}, ν_{21} = Poisson's ratios

3.2.2 Strain Displacement Relations

The linear strains are defined as follows

$$\varepsilon_x = \frac{\partial u}{\partial x} + z\kappa_x, \varepsilon_y = \frac{\partial v}{\partial y} + z\kappa_y, \gamma_{xy} = \frac{\partial u}{\partial y} + \frac{\partial v}{\partial x} + z\kappa_{xy},$$

$$\kappa_x = \frac{\partial \theta_x}{\partial x}, \kappa_y = \frac{\partial \theta_y}{\partial y}, \kappa_{xy} = \frac{\partial \theta_x}{\partial y} + \frac{\partial \theta_y}{\partial x}$$

$$\gamma_{xz} = \theta_x + \frac{\partial w}{\partial x}, \gamma_{yz} = \theta_y + \frac{\partial w}{\partial y} \tag{5}$$

The nonlinear strain components are defined as follows:

$$\varepsilon_{xnl} = \frac{1}{2}\left(\frac{\partial u}{\partial x}\right)^2 + \frac{1}{2}\left(\frac{\partial v}{\partial x}\right)^2 + \frac{1}{2}\left(\frac{\partial w}{\partial x}\right)^2 + \frac{1}{2}z^2\left[\left(\frac{\partial \theta_x}{\partial x}\right)^2 + \left(\frac{\partial \theta_y}{\partial x}\right)^2\right]$$

$$\varepsilon_{ynl} = \frac{1}{2}\left(\frac{\partial u}{\partial y}\right)^2 + \frac{1}{2}\left(\frac{\partial v}{\partial y}\right)^2 + \frac{1}{2}\left(\frac{\partial w}{\partial y}\right)^2 + \frac{1}{2}z^2\left[\left(\frac{\partial \theta_x}{\partial y}\right)^2 + \left(\frac{\partial \theta_y}{\partial y}\right)^2\right]$$

$$\gamma_{xnl} = \left(\frac{\partial u}{\partial x}\right)\left(\frac{\partial u}{\partial y}\right) + \left(\frac{\partial v}{\partial x}\right)\left(\frac{\partial v}{\partial y}\right) + \left(\frac{\partial w}{\partial x}\right)\left(\frac{\partial w}{\partial y}\right) + z^2\left[\left(\frac{\partial \theta_x}{\partial x}\right)\left(\frac{\partial \theta_y}{\partial y}\right) + \left(\frac{\partial \theta_y}{\partial x}\right)\left(\frac{\partial \theta_x}{\partial y}\right)\right]$$

Green's non-linear strains are used for derivation of geometrics stiffness matrix due to hygrothermal loads.

u, v, w = displacements of the mid-plane along x, y and z axes respectively

θ_x, θ_y = rotations of the plate about x and y axes

3.3 Buckling of Composite Plate

The problem considered here consists of a composite plates of length 'a' and width 'b' consisting of n number of thin homogeneous arbitrarily oriented orthotropic layers having a total thickness 'h' subjected to in-plane localized compressive edge loadings as shown in Figure 3. The angle θ measured in the anti-clockwise direction of x-axis represents the fiber orientation.

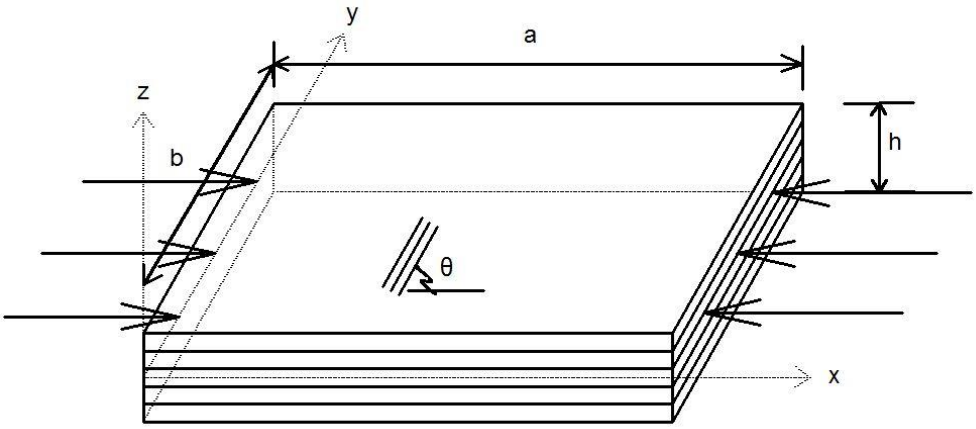

Figure 3 - Laminated Composite Plate under In-Plane Compression

The governing differential equations of equilibrium for buckling of laminated composite plate subjected to in-plane external in-plane loading can be written as:

$$\frac{\partial N_x}{\partial x} + \frac{\partial N_{xy}}{\partial y} = P_1 \frac{\partial^2 u}{\partial t^2} + P_2 \frac{\partial^2 \theta_x}{\partial t^2}$$

$$\frac{\partial N_{xy}}{\partial x} + \frac{\partial N_y}{\partial y} = P_1 \frac{\partial^2 v}{\partial t^2} + P_2 \frac{\partial^2 \theta_y}{\partial t^2}$$

$$\frac{\partial Q_x}{\partial x} + \frac{\partial Q_y}{\partial y} + N_x{}^0 \frac{\partial^2 w}{\partial x^2} + N_y{}^0 \frac{\partial^2 w}{\partial y^2} = P_1 \frac{\partial^2 w}{\partial t^2}$$

$$\frac{\partial M_x}{\partial x} + \frac{\partial M_{xy}}{\partial y} - Q_x = P_3 \frac{\partial^2 \theta_x}{\partial t^2} + P_2 \frac{\partial^2 u}{\partial t^2}$$

$$\frac{\partial M_x}{\partial x} + \frac{\partial M_y}{\partial y} - Q_y = P_3 \frac{\partial^2 \theta_y}{\partial t^2} + P_2 \frac{\partial^2 v}{\partial t^2}$$

Where N_x, N_y, and N_{xy} are the internal forces in normal and tangential direction. Q_x and Q_y shearing forces and M_x, M_y and M_{xy} the moment resultants on laminate.

3.4 Finite element formulation

Eight-noded isoparametric element used for vibration analysis of woven fiber composite plates subjected to hygrothermal loading. Five degrees of freedom *u*, *v*, *w*, θ_x and θ_y are considered at each node. The stiffness matrix, the mass matrix and the nodal load vectors of the element are

derived by using the principle of minimum potential energy. The displacements are expressed in terms of their nodal values by using the element shape functions and are given by.

$$u = \sum_{i=1}^{8} N_i u_i , v = \sum_{i=1}^{8} N_i v_i , w = \sum_{i=1}^{8} N_i w_i \qquad (6)$$

$$\theta_x = \sum_{i=1}^{8} N_i \theta_{xi} , \theta_y = \sum_{i=1}^{8} N_i \theta_{yi}$$

$N_i =$ Shape function at a node i

The shape function N_i are defined as

$$N_i = \frac{1}{4}(1+\xi\xi_i)(1+\eta\eta_1)(\xi\xi_1 + \eta\eta_1 - 1) \qquad \text{For } i = 1, 2, 3 \text{ \& } 4$$

$$N_i = \frac{1}{2}(1-\xi^2)(1+\eta\eta_i) \qquad \text{For } i = 5, 7$$

$$N_i = \frac{1}{2}(1-\xi\xi_i)(1-\eta^2) \qquad \text{For } i = 6, 8$$

$\xi, \eta =$ Local natural co-ordinates of an element

3.4.1 Element stiffness matrix

The linear strain matrix $\{\varepsilon\}$ is expressed as

$$\{\varepsilon\} = [B]\{\delta_e\} \qquad (7)$$

Where $\{\delta_e\} = \{u_1, v_1, w, \theta_{x1}, \theta_{y1} ....., u_8, v_8, w_8 \theta_{x8}, \theta_{y8}\}^T$,

$$[B] = \sum_{i=1}^{8} \begin{bmatrix} N_{i,x} & 0 & 0 & 0 & 0 \\ 0 & N_{i,y} & 0 & 0 & 0 \\ N_{i,y} & N_{i,x} & 0 & 0 & 0 \\ 0 & 0 & 0 & 0 & N_{i,x} \\ 0 & 0 & 0 & N_{i,y} & 0 \\ 0 & 0 & 0 & N_{i,x} & N_{i,y} \\ 0 & 0 & N_{i,x} & 0 & N_i \\ 0 & 0 & N_{i,y} & N_i & 0 \end{bmatrix}$$

Element stiffness matrix is given by

$$[K_e] = \int_{-1}^{+1}\int_{-1}^{+1} [B]^T [D][B] J | d\xi d\eta \qquad (8)$$

3.4.2 Element initial stress stiffness matrix

The non-linear strain equations are represented in matrix form:

$$\varepsilon_{nl} = \left\{\varepsilon_{xnl}, \varepsilon_{ynl}, \gamma_{xynl}\right\}^T = [R]\{d\}/2$$

Where $$\{d\} = \left\{u_x, u_y, v_x, v_y, w_x, w_y, \theta_{x,x}, \theta_{x,y}, \theta_{y,x}, \theta_{y,y}, \theta_x, \theta_y\right\}^T$$

Equations $\{d\}$ may be expressed as:

$$\{d\} = \{G\}\{\partial_e\} \tag{9}$$

Where $$[G] = \sum_{i=1}^{8} \begin{bmatrix} N_{i,x} & 0 & 0 & 0 & 0 \\ N_{i,y} & 0 & 0 & 0 & 0 \\ 0 & N_{i,x} & 0 & 0 & 0 \\ 0 & N_{i,y} & 0 & 0 & 0 \\ 0 & 0 & N_{i,x} & 0 & 0 \\ 0 & 0 & N_{i,y} & 0 & 0 \\ 0 & 0 & 0 & N_{i,x} & 0 \\ 0 & 0 & 0 & N_{i,y} & 0 \\ 0 & 0 & 0 & 0 & N_{i,x} \\ 0 & 0 & 0 & 0 & N_{i,y} \\ 0 & 0 & 0 & 1 & 0 \\ 0 & 0 & 0 & 0 & 1 \end{bmatrix}$$

The initial stress stiffness matrix due to hygrothermal loads are given by:

$$\left[K_{\sigma e}\right] = \int_{-1}^{+1}\int_{-1}^{+1} [G]^T [S][G] J \left| d\xi d\eta \right. \tag{10}$$

Where

$$[S] = \begin{bmatrix} S_{11} & & & & & & & & & & & \\ S_{21} & S_{22} & & & & & & & & & & \\ 0 & 0 & S_{33} & & & & & & & & & \\ 0 & 0 & S_{43} & S_{44} & & & & & & & & \\ 0 & 0 & 0 & 0 & S_{55} & & & & & & & \\ 0 & 0 & 0 & 0 & S_{65} & S_{66} & & & & & & \\ 0 & 0 & S_{73} & S_{74} & 0 & 0 & S_{77} & & & & & \\ 0 & 0 & S_{83} & S_{84} & 0 & 0 & S_{87} & S_{88} & & & & \\ S_{91} & S_{92} & 0 & 0 & 0 & 0 & 0 & 0 & S_{99} & & & \\ S_{101} & S_{102} & 0 & 0 & 0 & 0 & 0 & & S_{109} & S_{110} & & \\ 0 & 0 & S_{113} & S_{114} & 0 & 0 & 0 & 0 & 0 & 0 & 0 & \\ S_{121} & S_{122} & 0 & 0 & 0 & 0 & 0 & 0 & 0 & 0 & 0 & 0 \end{bmatrix}$$

In which

$S_{11} = S_{33} = S_{55} = N^r{}_x \qquad S_{22} = S_{44} = S_{66} = N^r{}_y$

$S_{21} = S_{43} = S_{65} = N^r{}_{xy}, \qquad S_{77} = S_{99} = N_x{}^r\ t^2/12, \qquad S_{88} = S_{1010} = N_y{}^r\ t^2/12$

$S_{87} = S_{109} = N^r{}_{xy} t^2/12, \qquad -S_{73} = S_{91} = M^r{}_x, \qquad -S_{84} = S_{102} = M^r{}_y$

$-S_{74} = -S_{83} = S_{92} = S_{101} = M^r{}_{xy}, \quad -S_{113} = S_{121} = Q^r{}_x, \quad -S_{114} = S_{122} = Q^r{}_y$

$N^{ir}{}_x, N^r{}_y, N^r{}_{xy}$ = in-plane initial internal force resultants per unit length

$M^r{}_x, M^r{}_y, M^r{}_{xy}$ = initial internal moment resultants per unit length

$Q^r{}_x, Q^r{}_y$ = initial transverse shear resultants

3.4.3 Element mass matrix

$$[M_e] = \int_{-1}^{+1}\int_{-1}^{+1} [N]^T [P][N] J\, d\xi d\eta \qquad (11)$$

Where the shape function matrix

$$[N] = \sum_{i=1}^{8} \begin{bmatrix} N_i & 0 & 0 & 0 & 0 \\ 0 & N_i & 0 & 0 & 0 \\ 0 & 0 & N_i & 0 & 0 \\ 0 & 0 & 0 & N_i & 0 \\ 0 & 0 & 0 & 0 & N_i \end{bmatrix}$$

$$[P_1] = \begin{bmatrix} P_1 & 0 & 0 & 0 & 0 \\ 0 & P_1 & 0 & 0 & 0 \\ 0 & 0 & P_1 & 0 & 0 \\ 0 & 0 & 0 & I & 0 \\ 0 & 0 & 0 & 0 & I \end{bmatrix}$$

In which, $\quad P_1 = \sum_{k=1}^{n} \int_{ek-1}^{ek} \rho dz \qquad$ And $\qquad I = \sum_{K=1}^{n} \int_{ek-1}^{ek} z^2 \rho dz$

The element load vector due to external transverse static load p per unit area is given by

$$\{P_e\} = \iint N_i \begin{bmatrix} p \\ 0 \\ 0 \end{bmatrix} dxdy \,. \qquad (12)$$

The element load vector due to hygrothermal forces and moments is given by

$$\{P^N\} = \int_{-1}^{+1}\int_{-1}^{+1} [B]^T \{F^N\} |J| d\xi d\eta \qquad (13)$$

3.4.4 Geometric stiffness matrix

Element geometric stiffness matrix $[K_g]_e = \int_{-1}^{+1}\int_{-1}^{+1} [G]^T [S][G] |J| d\xi d\eta \qquad (14)$

$$[G] = \begin{bmatrix} N_{i,x} & 0 & 0 & 0 & 0 \\ N_{i,y} & 0 & 0 & 0 & 0 \\ 0 & N_{i,x} & 0 & 0 & 0 \\ 0 & N_{i,y} & 0 & 0 & 0 \\ 0 & 0 & N_{i,x} & 0 & 0 \\ 0 & 0 & N_{i,y} & 0 & 0 \\ 0 & 0 & 0 & N_{i,x} & 0 \\ 0 & 0 & 0 & N_{i,y} & 0 \\ 0 & 0 & 0 & 0 & N_{i,x} \\ 0 & 0 & 0 & 0 & N_{i,y} \end{bmatrix} \text{ and } [S] = \begin{bmatrix} s & 0 & 0 & 0 & 0 \\ 0 & s & 0 & 0 & 0 \\ 0 & 0 & s & 0 & 0 \\ 0 & 0 & 0 & s & 0 \\ 0 & 0 & 0 & 0 & s \end{bmatrix}$$

Where as $[s] = \begin{bmatrix} \sigma_x & \tau_{xy} \\ \tau_{xy} & \sigma_y \end{bmatrix} = \frac{1}{h} \begin{bmatrix} N_x & N_{xy} \\ N_{xy} & N_y \end{bmatrix}$

The in-plane stress resultants N_x, N_y, N_{xy} at each gauss point are obtained by applying uniaxial stress in x-direction.

3.5 Vibration Analysis

The first part of the solution is to obtain the initial stress resultants induced by the moisture and temperature conditions. The element stiffness matrix, the initial stress stiffness matrix due to hygrothermal load, the mass matrix and the load vectors of the element, given by equations (10)-(14), are evaluated by first expressing the integrals in local Natural co-ordinates, ξ and η of the element and then performing numerical integration by using Gaussian quadrature.

The initial displacements $\{\delta^i\}$, are found the equilibrium condition

$$[K]\{\delta^i\} = \{P^N\} \tag{15}$$

Then the initial stress resultants $N^i{}_x, N_y{}^i, N^i{}_{xy}, M^i{}_x, M^i{}_y, M^i{}_{xy}, Q^i{}_x$ and $Q^i{}_y$ are obtained from equations (1) and (10). Then the element matrices are assembled to obtain the respective global matrices $[K], [K_\sigma]$ and $[M]$. The next part of the solution involves determination of natural frequencies from the eigenvalue solution of the equation given below.

$$\text{For vibration} \qquad [K] + [K_\sigma] - \omega_n{}^2 \quad [M] = 0 \tag{16}$$

3.6 Buckling Analysis

The governing equation for buckling analysis of woven fiber laminated composite plate is

$$[[K] - P\,[K_g]]\,[q] = \{0\} \tag{17}$$

Where [K] and $[K_g]$ are the bending and geometric stiffness matrix and [q] is the vector of degrees of freedoms

3.7 Computer Program

Based on the above finite element formulation on thermal analysis with modeling of laminated composite plates, codes are developed in MATLAB environment to compute the free vibration response of industry driven woven fibre Glass/Epoxy composite plates exposed to thermal environment. The formulation can handle any geometry, material and general distribution of temperature.

CHAPTER -4

EXPERIMENTAL PROGRAMME

The experimental investigation describes in detail of the materials and its fundamental constituents, the fabrication of composite plates, and the test methods according to standards.

4.1 Fabrication Method

Specimens were cast using hand layup technique as shown in Figure 4. In hand lay-up method, liquid resin was placed along with industry driven woven carbon fiber against finished surface of an open mould. The percentage of fiber and matrix was taken as 50:50 in weight for fabrication of the plates as per ASTM-D5678M-07. Lamination started with the application of a gel coat made up of epoxy resin and 8% hardener (Ciba-Geigy, Araldite HY556 and Hardener HY951) deposited on the mould by brush. Layers of reinforcement consisting of woven roving glass fibers manufactured by Owens Corning, weighing 360 g/m^2 and carbon fibers (8H SATIN, T-300) manufactured by TORAY industry, weighing 420 g/m^2 were placed on the mould at top of the gel coat and gel coat was applied again by brush. Any air which may be entrapped was removed using steel rollers. After completion of all layers, again a plastic sheet was covered the top of last ply by applying polyvinyl alcohol inside the sheet as releasing agent. Again one flat ply board and a heavy flat metal rigid platform were kept top of the plate for compressing purpose. The plates were left for a minimum of 48 hours in room temperature before being transported and cut to exact shape for testing. In case of hybrid plates of glass fibre and carbon fibre layers are laid as per the required sequence.

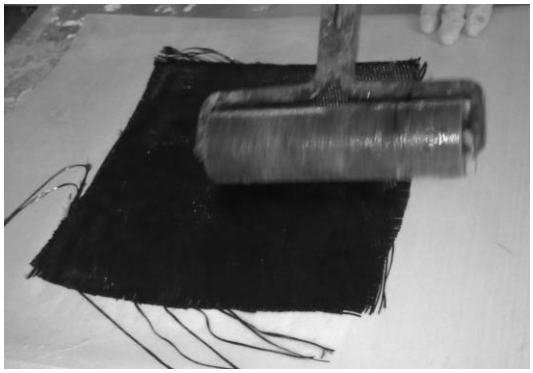

Figure 4 - Hand Lay-up technique

4.2 Determination of Physical Properties

The physical properties of fabricated composite plates such as density and thickness, represented in Table 1 and 2, were measured up to the required degree of accuracy. The thickness was measured using vernier caliper with a least count of 0.1 mm. The weight of the specimen was measured using digital weighing balance with an accuracy of 0.1 grams.

Table 1- Physical properties of the casted carbon fibre specimens

Sl. No.	No of layers	Length in m	Width in m	Thickness in m	Mass in g	Density in kg/m3
1	4	0.24	0.24	0.0021	174	1438.49
2	8	0.24	0.24	0.0042	345	1426.09
3	12	0.24	0.24	0.0065	519	1386.22
4	8	0.10	0.10	0.0042	60	1428.57

Table 2- Physical properties of the casted carbon-glass hybrid specimens

Sl. No.	% of Carbon fiber	Lamination Sequence	No of layers	Length in m	Width in m	Thickness in m	Mass in g	Density in kg/m3
1	25	$[C\text{-}G\text{-}G\text{-}G]_s$	8	0.20	0.20	0.0033	205	1608
2	25	$[G\text{-}C\text{-}G\text{-}G]_s$	8	0.20	0.20	0.0031	196	1596
3	25	$[G\text{-}G\text{-}C\text{-}G]_s$	8	0.20	0.20	0.0034	213	1621
4	25	$[G\text{-}G\text{-}G\text{-}C]_s$	8	0.20	0.20	0.0033	218	1685
5	50	$[C\text{-}C\text{-}G\text{-}G]_s$	8	0.20	0.20	0.0036	223	1549
6	50	$[G\text{-}G\text{-}C\text{-}C]_s$	8	0.20	0.20	0.0035	215	1536
7	50	$[C\text{-}G\text{-}C\text{-}G]_s$	8	0.20	0.20	0.0036	223	1549

4.3 Tensile tests of the specimen

The Young's modulus was obtained experimentally by performing unidirectional tensile tests on specimens cut in longitudinal and transverse directions as described in ASTM-D3039M-08 from the FRP plates fabricated earlier. Strips of specimens having a constant rectangular cross-section, say 250 mm long × 25mm width are prepared from the plates. Three or more sample specimens were prepared from each plate of CFRP in this experiment. The specimen is gradually loaded up to failure, which was abrupt and sudden as the FRP material was brittle in nature. The INSTRON 1195 machine as shown in Figure 5 directly indicated the Young's Modulus, ultimate strength.

Figure 5 - Tensile testing of CFRP plates using INSTRON 1195

4.4 Experimental investigation of vibration of woven fiber composite plates:

4.4.1. Hygrothermal Treatment:

The composite specimen were thermally treated in temperature bath and temperature/humidity chamber separately and then allowed to return to room temperature to study the effect of temperature variation and elevated moisture concentration of carbon fibre composites on natural frequencies of vibration.

For maintaining a particular moisture concentration in a specimen, the oven dried samples were kept in humidity chamber at a specified temperature and relative humidity according to the requirements of ASTM-D5229M-04 for moisture absorption. The moisture uptake of the sample was recorded by periodically removing it from the temperature/humidity chamber and allowing it to cool in a sealed, humid environment. The weight of the sample was immediately recorded and was quickly kept back in the chamber for further increase in moisture concentration. The present

investigation was conducted for various moisture concentrations. The formula used for calculation of moisture content as per ASTM-D5229M-04 is as follows:

$$M, \% = [(W_i - W_0)/W] * 100 \quad (18)$$

Where M is the moisture content of the specimen in %, W_i is the current specimen mass in g, and W_0 is the oven-dry specimen mass in g.

For studying the effect of temperature variation six different temperatures as 223 K, 248 K, 273 K, 298 K, 323 K and 348 K were chosen. Cryogenic temperature was reached by cooling the specimen in low temperature chamber in the presence of silica gel to avoid moisture absorption by the specimen, as shown in figure 6. Higher temperatures were obtained using high temperature oven. The samples were first kept in temperature bath for 8 hours and then allowed to cool at room temperature, before testing.

Figure 6 - Carbon fibre composite plate in Ultra Low Chamber for cryogenic temperature conditioning

4.4.2 Setup and Test Procedure for free vibration test of composite plates:

The connections of FFT analyzer, laptop, transducers, modal hammer, and cables to the system were done as per the guidance manual. The pulse lab shop software key was inserted to the port of laptop. The plate was excited in a selected point by means of Impact hammer (Model 2302-5).

The resulting vibrations of the specimens on the selected point were measured by an accelerometer (B&K, Type 4507) mounted on the specimen by means of bees wax. The plates were placed as per the required boundary conditions. The various boundary conditions under study are as follows:

1. Free on all sides (FFFF)
2. Clamped on all edges (CCCC)
3. Simply supported on boundary (SSSS)
4. Clamped on one edge and free on the other three edges (CFFF)
5. Clamped on two opposite sides and simply supported on the other two sides (CSCS)

Figure 7 represents the experimental setup of the different boundary conditions for the vibration analysis of the laminates.

(a)

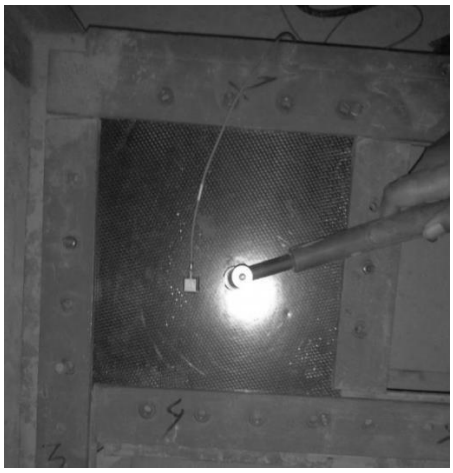

(b)

(c)

Figure 7 – Carbon fibre composite plate during testing for different support condition (a) free-free (b) fully clamped and (c) CSCS.

4.4.3 Setup and Test Procedure for Buckling Test:

A frame was fabricated to keep two opposite sides clamped and the other two sides in free condition. The specimen was loaded to failure in INSTRON 1195 by applying axial compression as can be seen from figure 8. The top and bottom edges were restrained against translation and rotation using clamping screws. For axial loading the specimen was placed between two extremely stiff machine heads. The lower machine head was fixed during the test and the upper head was moved downwards by servo-hydraulic cylinder. All plates were loaded at a constant crosshead speed of 0.5 mm/min. The compressive load versus compressive extension curve was plotted by the system connected to the machine, as shown in figure 9. The critical buckling load was determined at the point where the curve deviated from its linearity.

Figure 8 – Carbon fibre composite plate subjected to axial compression in INSTRON 1195

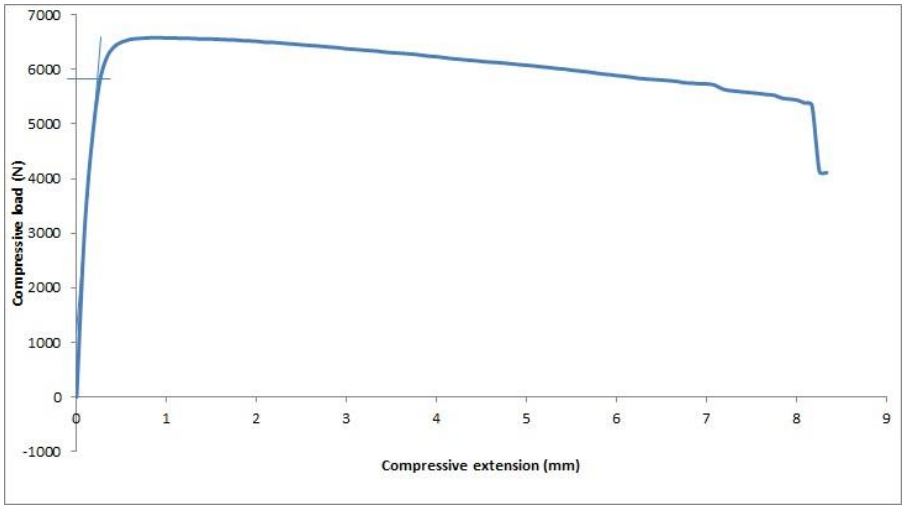

Figure 9 – Load versus end shortening curve for 4 layered CFRP plate in CFCF boundary condition

CHAPTER - 5

MODELING USING ANSYS 13.0

5.1 ANSYS Model

The CFRP plate was modeled using a commercially available finite element package, ANSYS 13.0 according to ANSYS user's manual. The natural frequencies and mode shapes are obtained by modal analysis. The element type used is SHELL281 which is an 8 noded structural shell, suitable for analyzing thin to moderately thick shell structures. The element has 8 nodes with 6 degrees of freedom at each node. The accuracy in modeling composite shells is governed by the first order shear deformation theory. The whole domain is divided into 8 x 8 meshes for all the cases. The boundary conditions of CCCC, CSCS, SSSS and CFFF were introduced by limiting the degrees of freedom at each node. FFFF condition was simulated by limiting displacement of the plate in vertical direction along the plane of plate. This condition closely resembled the experimental used in which the plate was hung vertically using strings of negligible stiffness.

5.2 Procedural steps for modeling

The procedural steps for modeling using ANSYS 13.0 are as follows:

1. Preferences → Structural →Ok

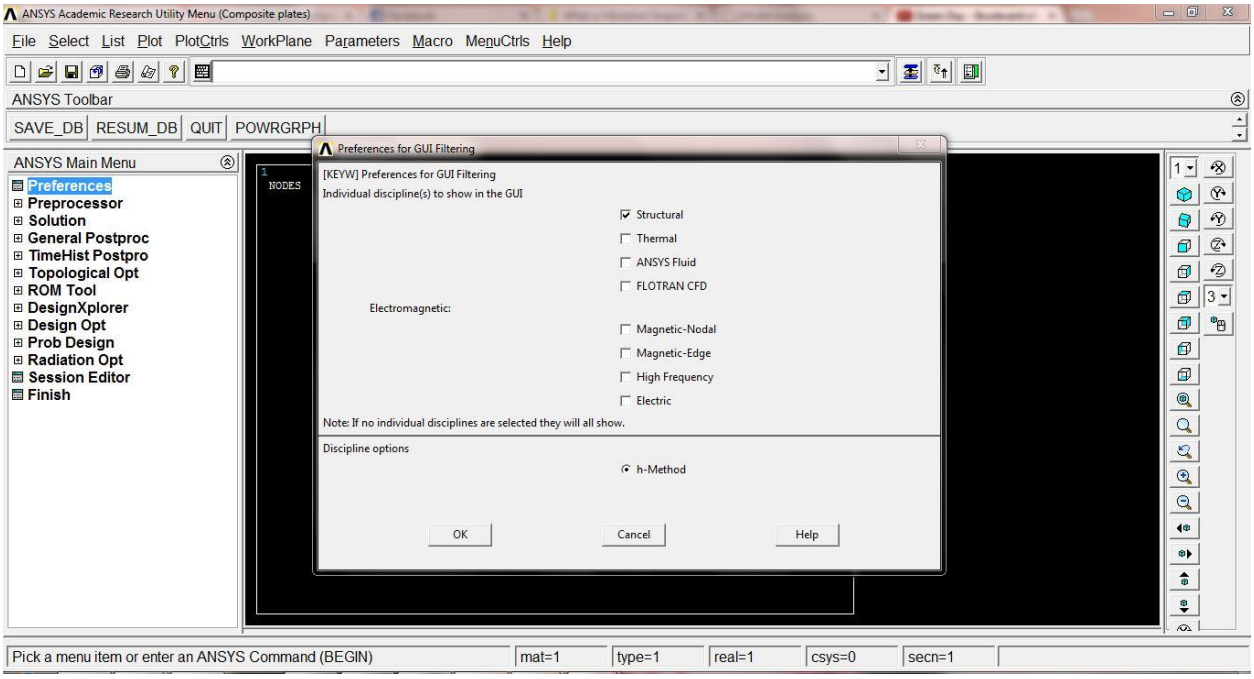

2. Preprocessor →Element type → Add → Structural Mass → Shell → 8node 281 → Ok

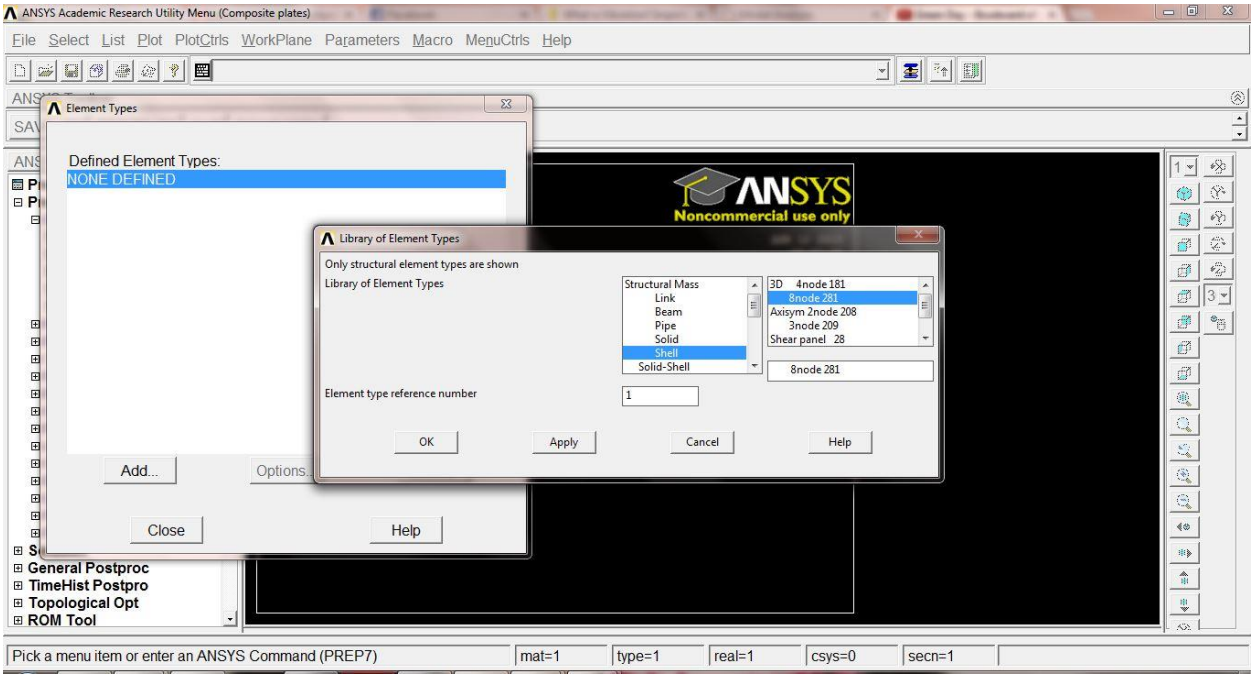

3. Select SHELL281 → Options → Storage of layer data – All layers → Ok

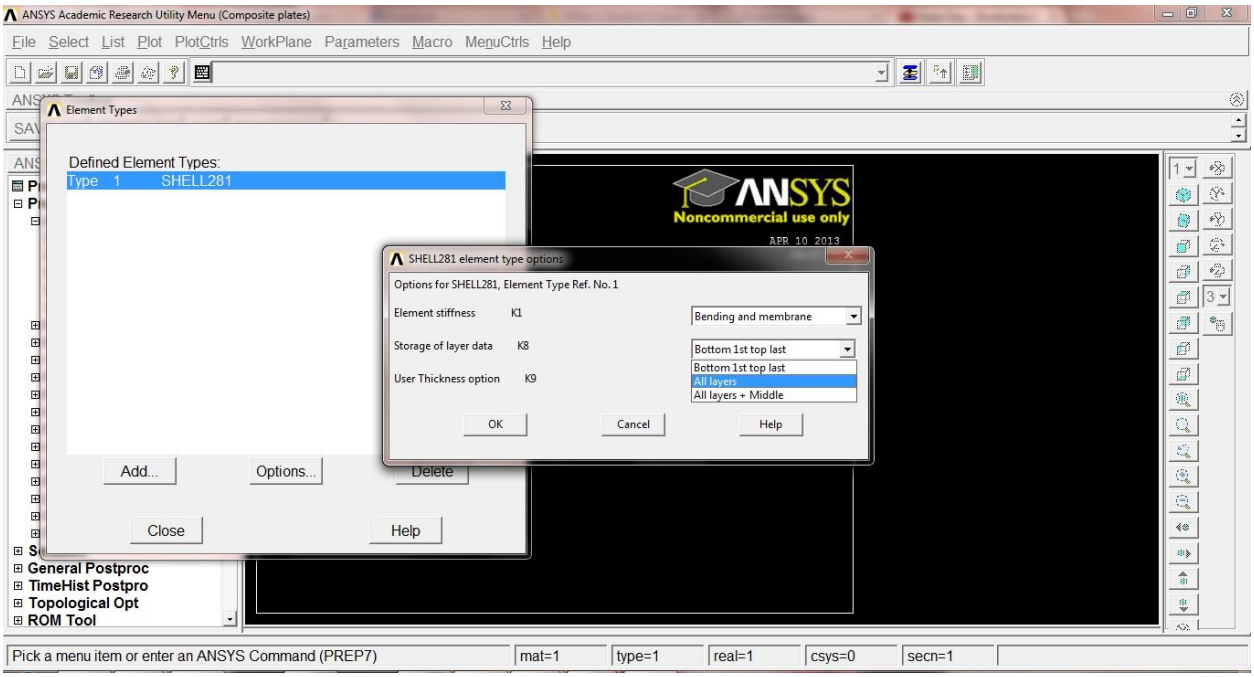

4. Preprocessor →Material Properties → Material Models → Structural → Linear → Elastic → Orthotropic

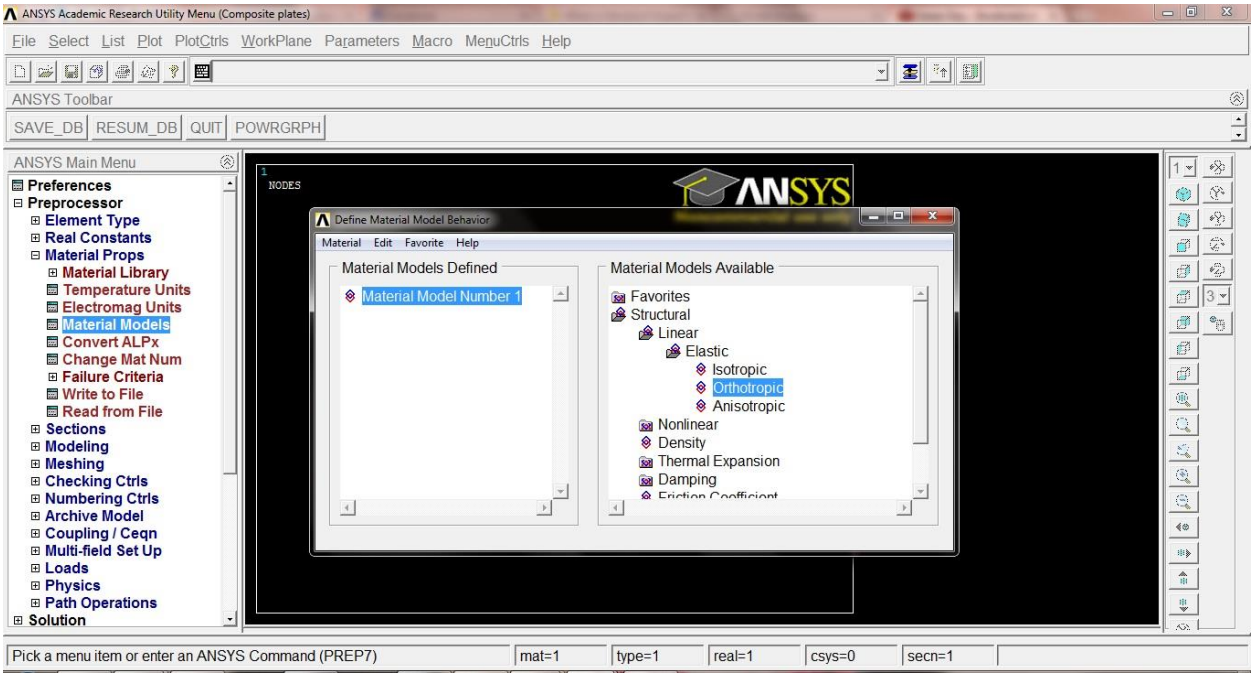

5. Enter the Linear Orthotropic Material Properties and press Ok.

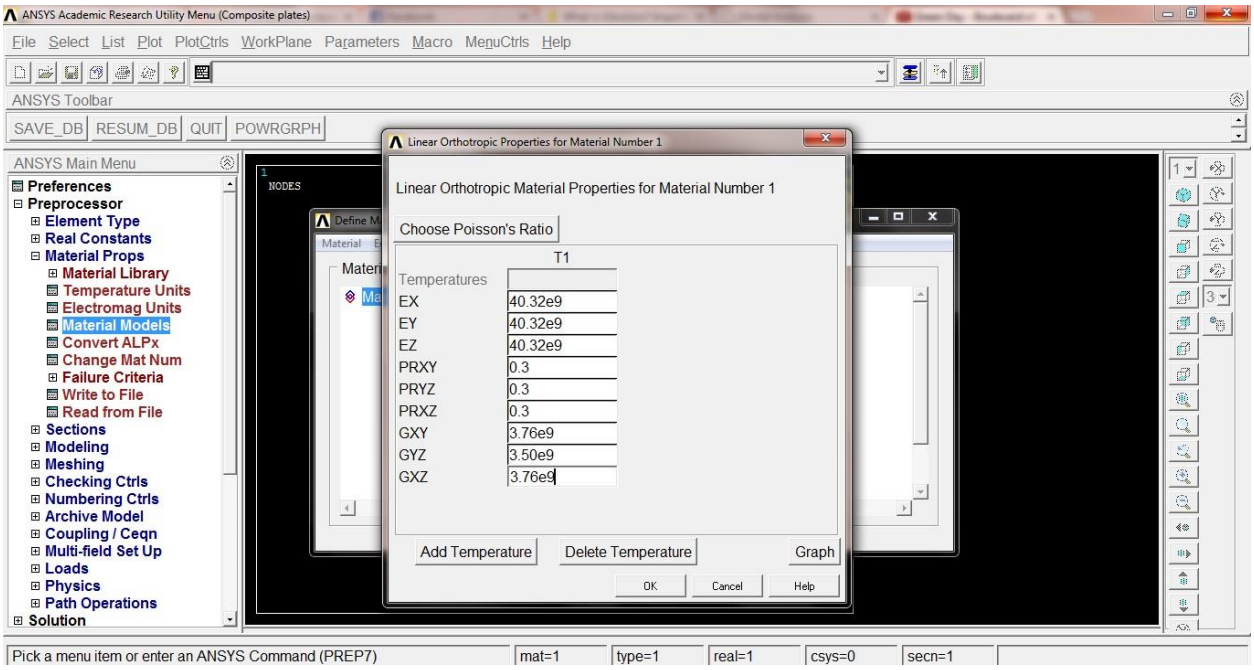

6. Material Models Available → Density → Enter the density of composite laminate → Ok

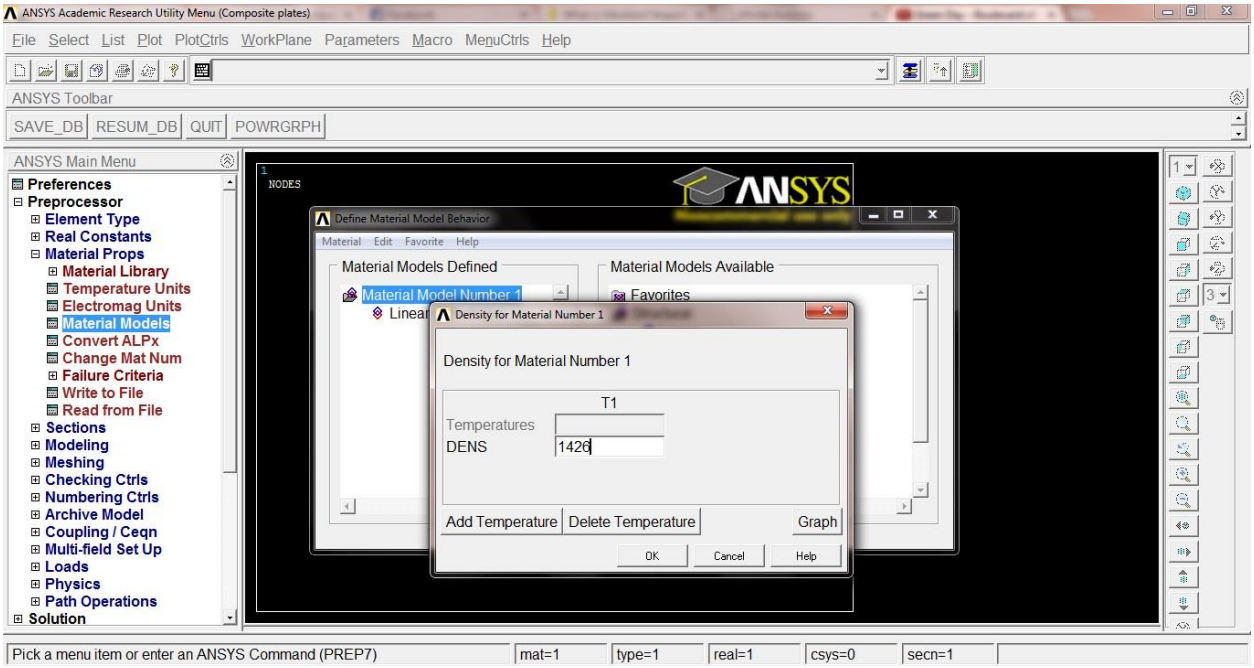

7. Preprocessor →Modeling → Create → Areas → Rectangle → By Dimensions → Enter the dimensions of the required plates → Ok

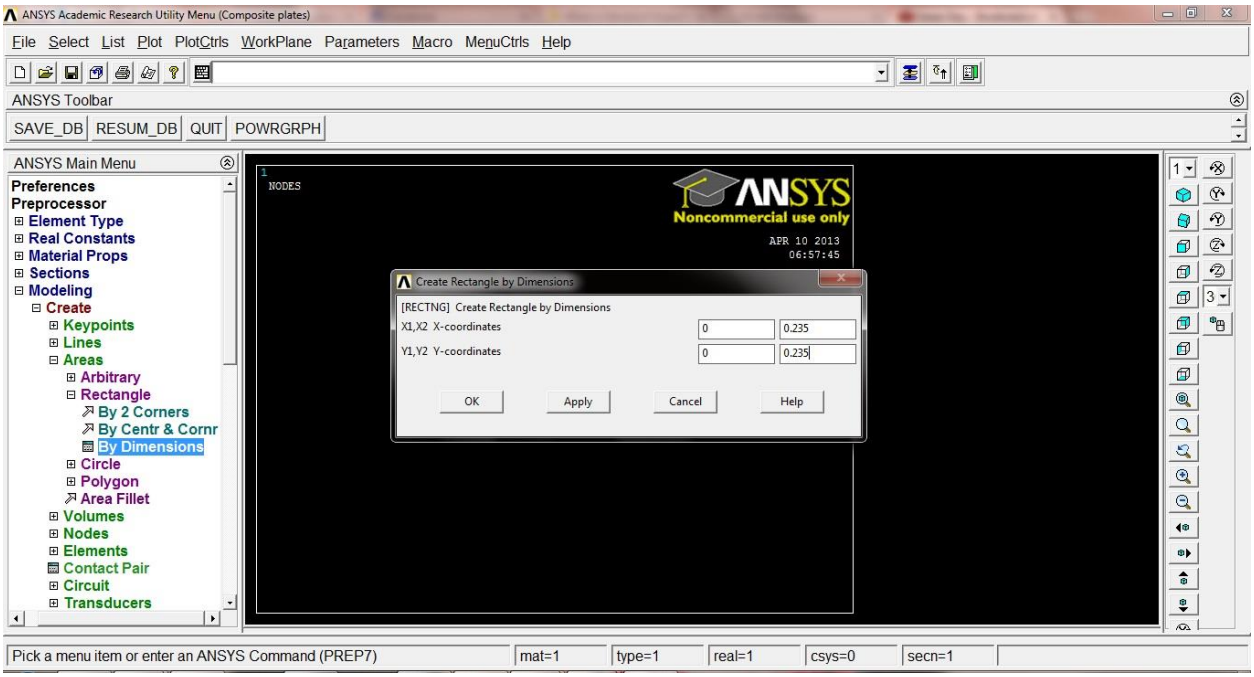

8. Preprocessor → Sections → Shell → Lay-up → Add/Edit → Enter thickness and orientation of each layer in the laminate by using Add Layer → Ok

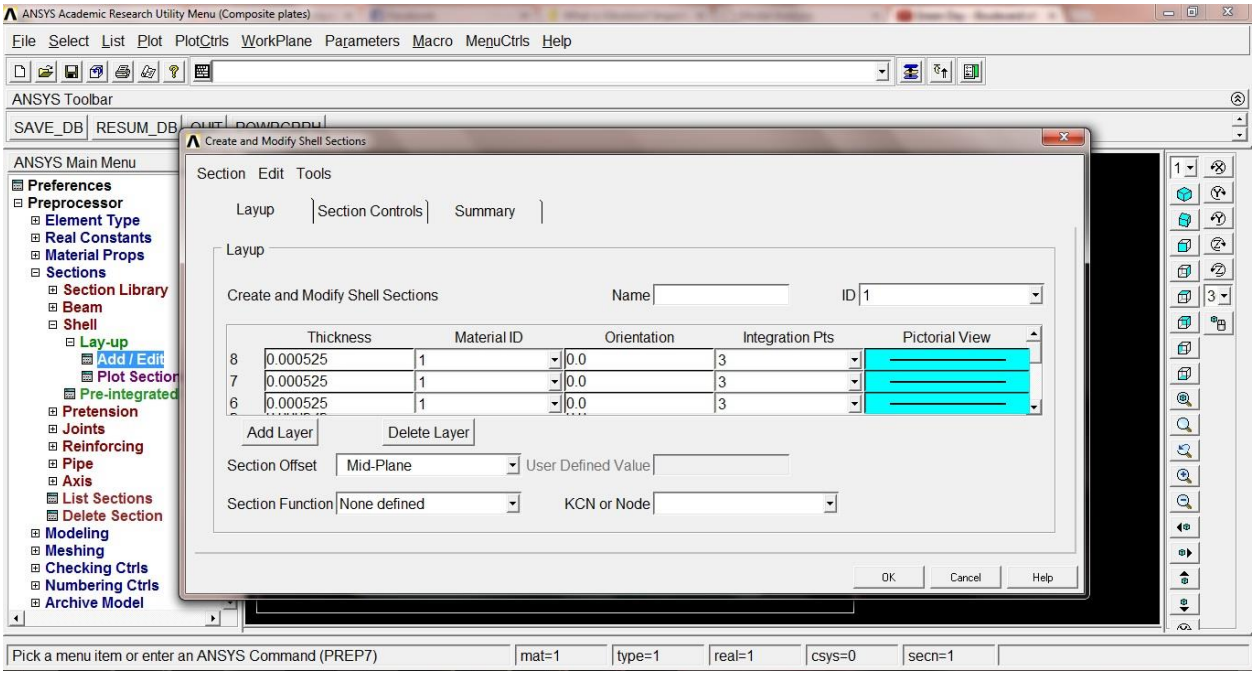

9. Preprocessor → Meshing → Mesh Tool → Size Controls: Global →Set → Enter no. of element divisions → Ok

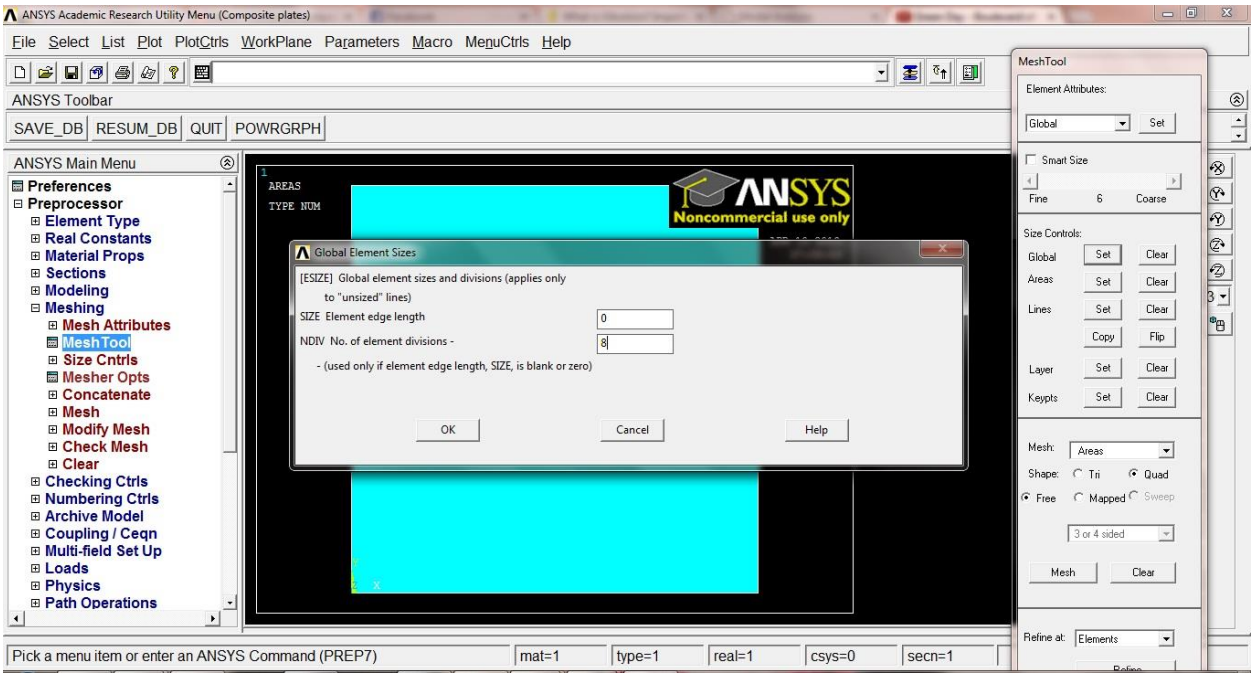

10. Preprocessor → Loads → Define Loads → Apply → Structural → Displacement → On Lines → Select the lines on which load is to be applied → Select the degree of freedom to be restrained according to the boundary condition → Ok

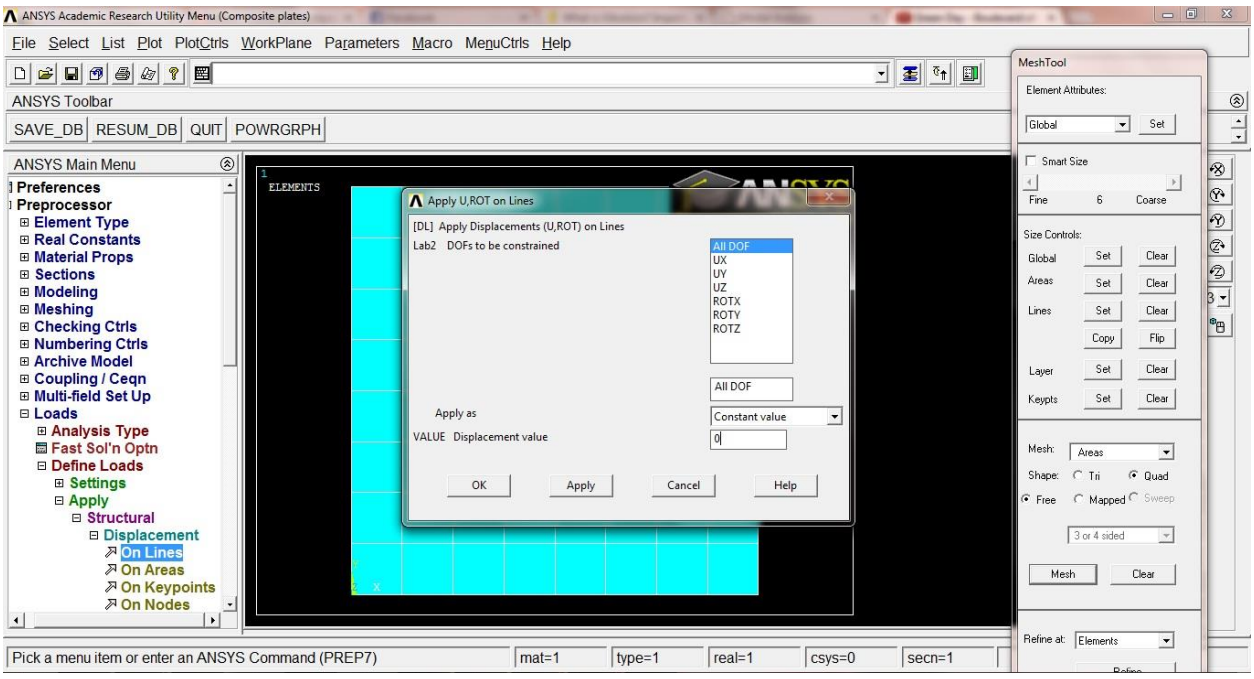

11. Preprocessor → Loads → Analysis Type → New Analysis → Type of analysis – Modal → Ok

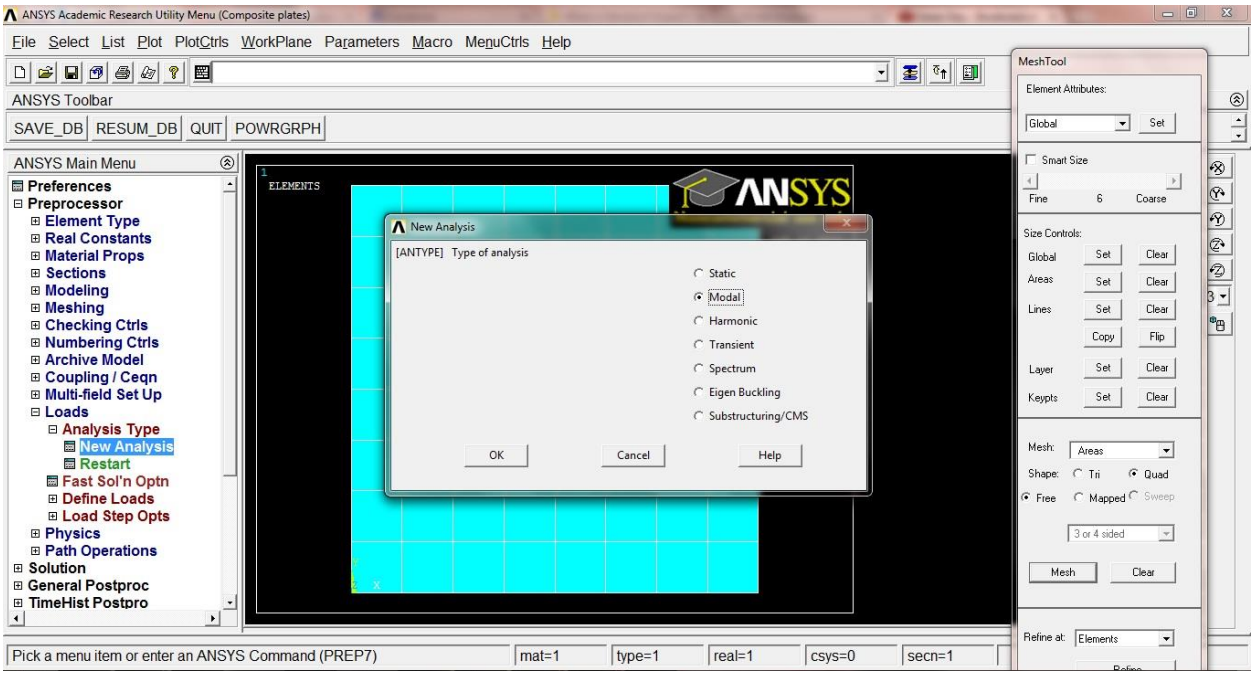

12. Preprocessor → Loads → Analysis Type → Analysis Options → Mode extraction method – Block Lanczos → No. of modes to extract - 10 → Ok

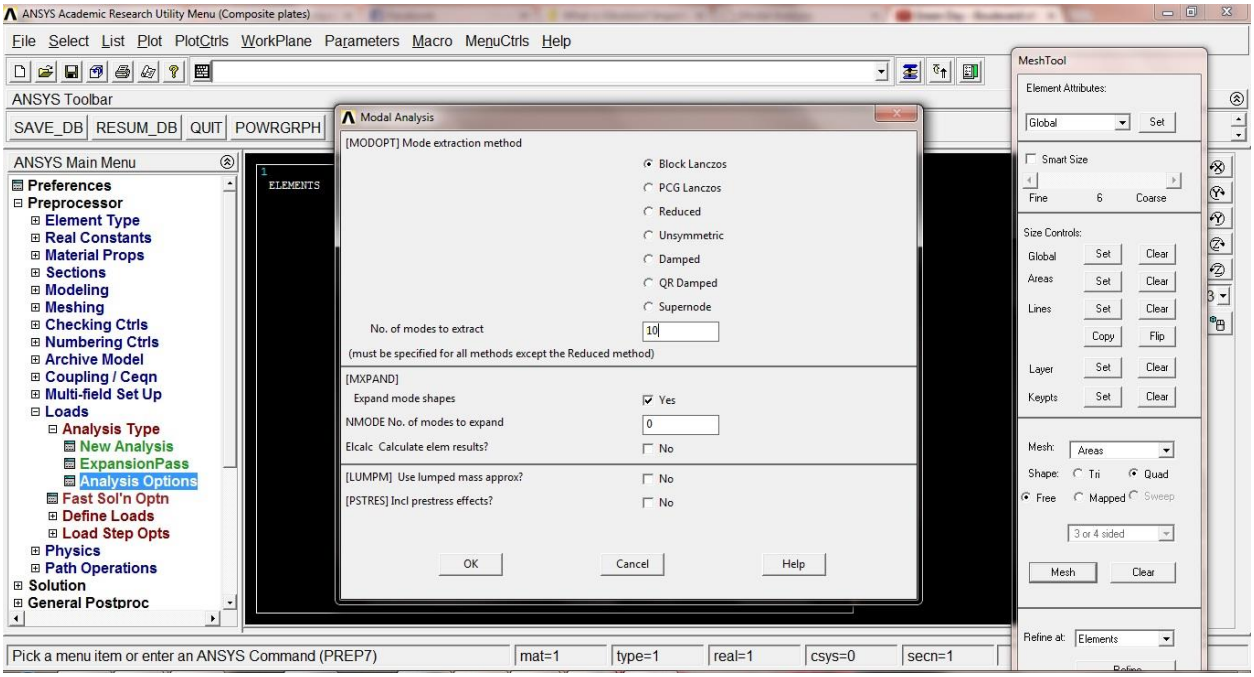

13. Block Lanczos Method → Enter the start and end frequency → Ok

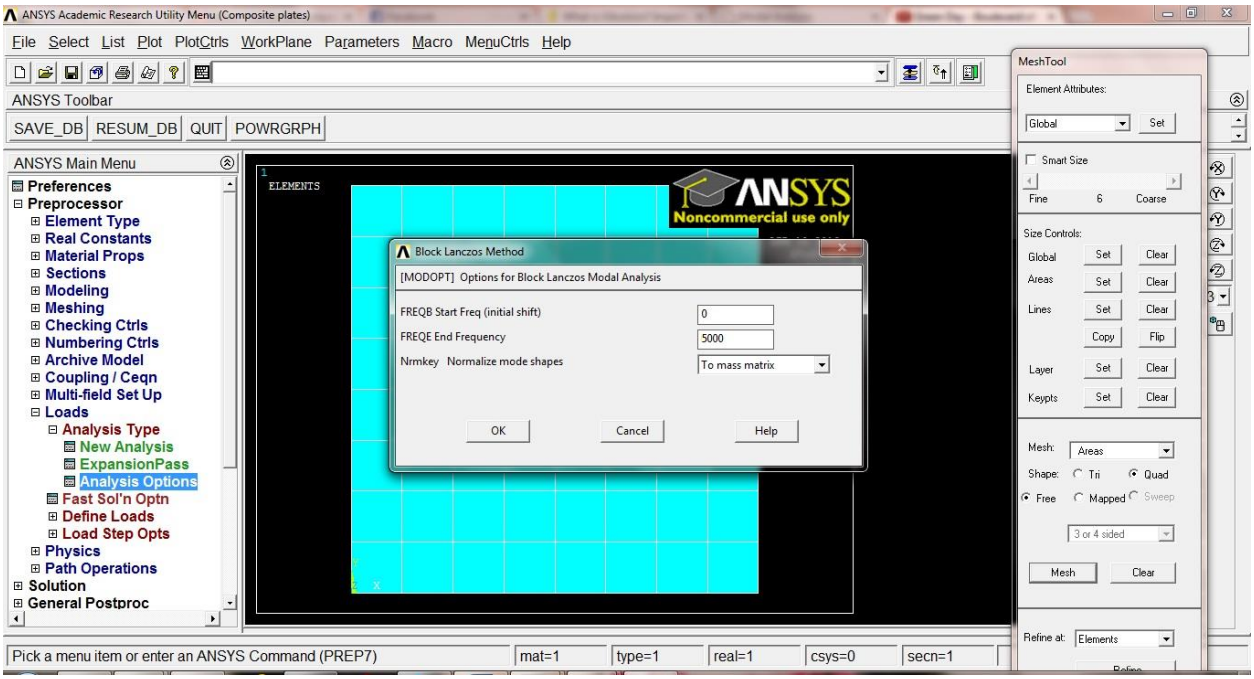

14. Solution → Solve → Current LS → Press ok in the Solve Current Load Step window

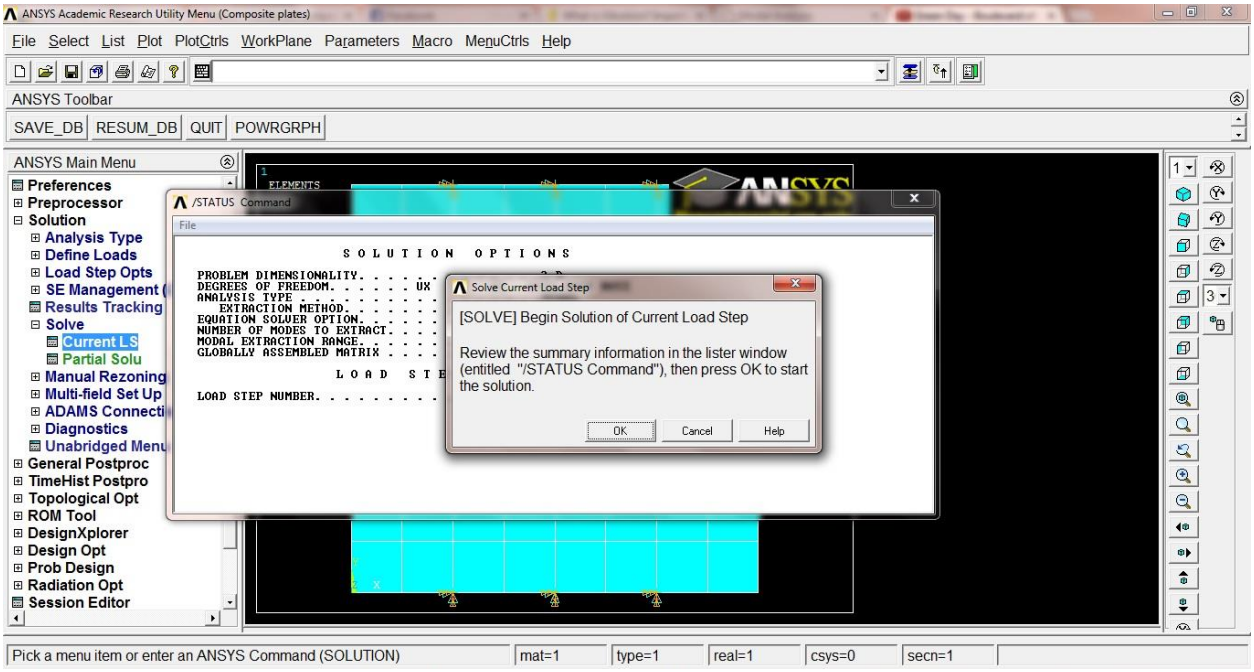

15. Once the solution is done a window displaying that solution is done is displayed. Cloase the window.

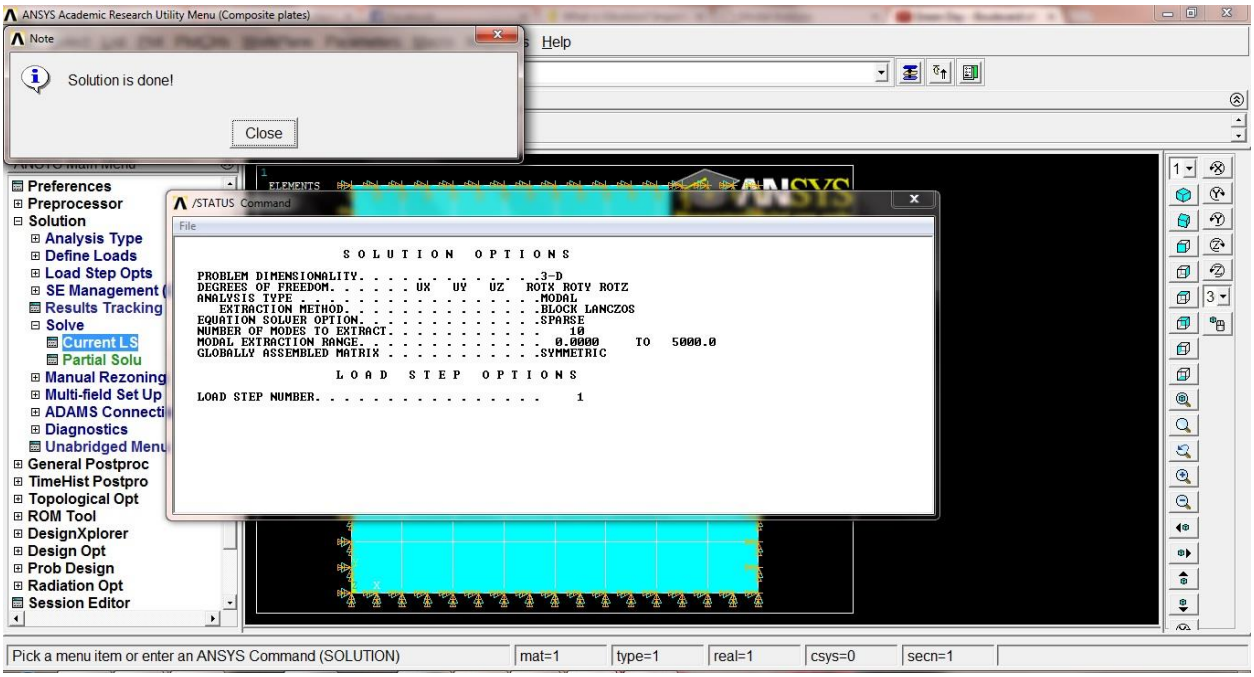

16. For viewing the results, follow the step given below:

General Postprocessing → Results Summary

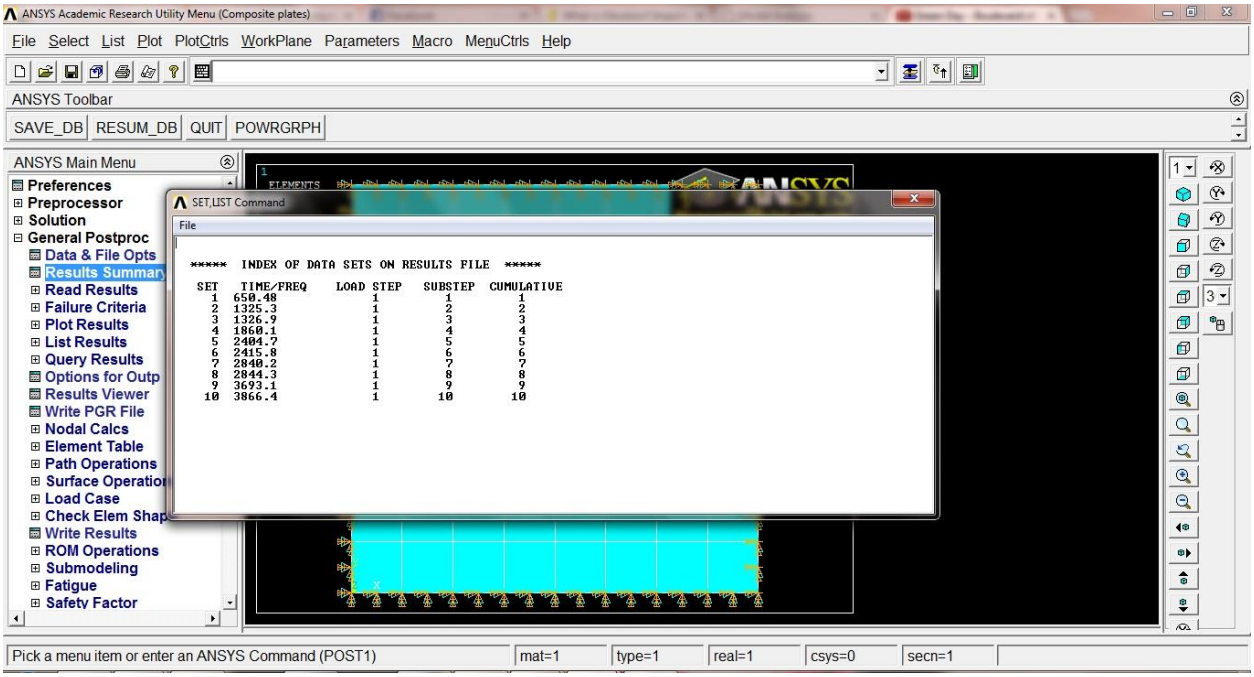

17. For viewing the deformed shape of the laminated composite plate the following steps should be followed:

General Postprocessing → Plot Results → Deformed Shape → Select the Items to be plotted → Ok

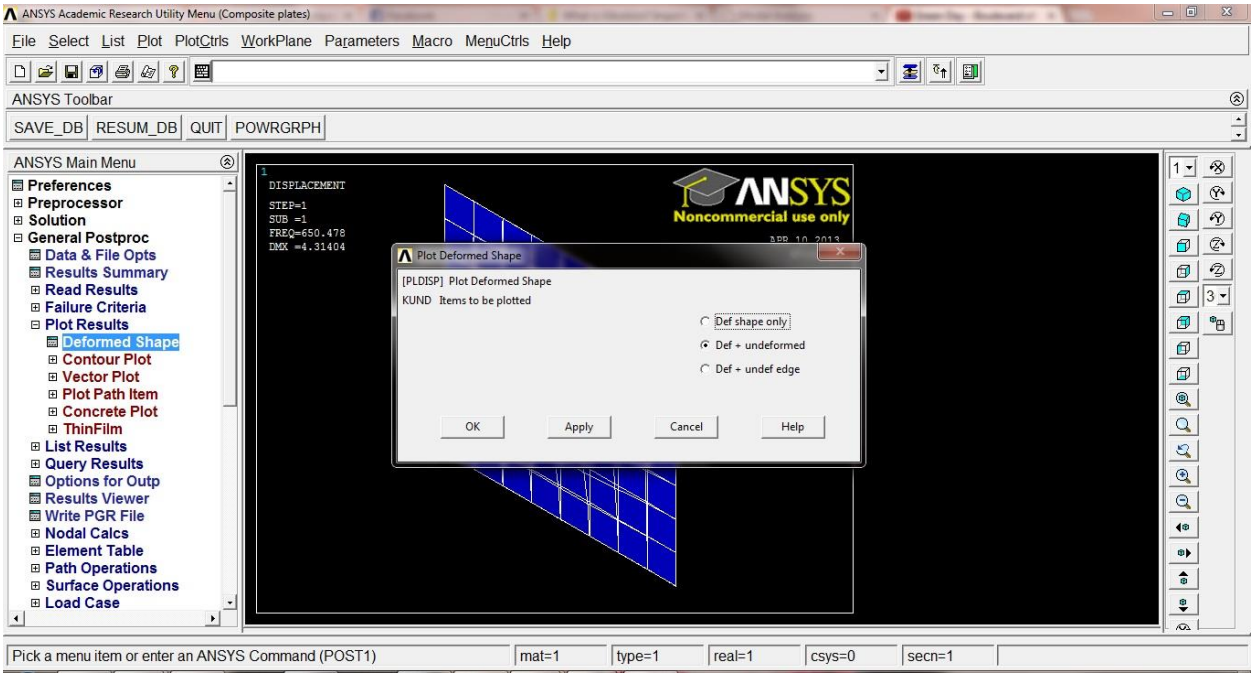

18. The plotted deformed shape will be as given below.

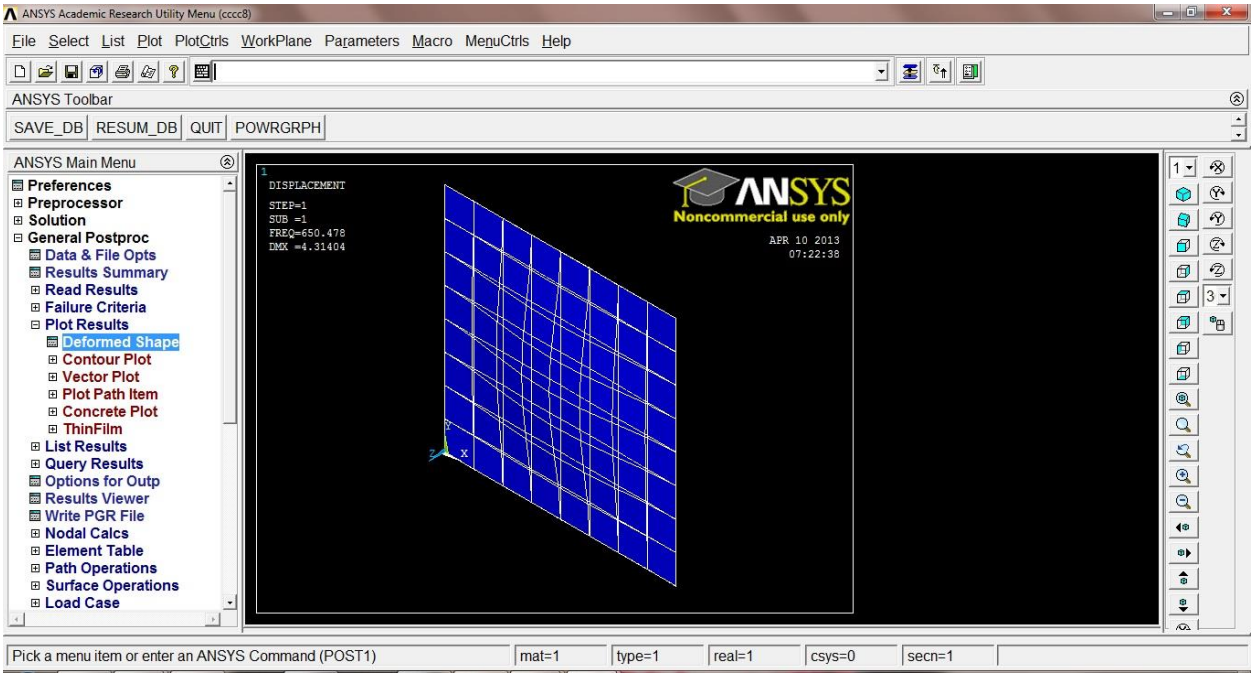

CHAPTER - 6

RESULTS AND DISCUSSION

6.1 Determination of material properties

The Young's moduli in longitudinal direction of the composite plates were determined as in Table 3. The transverse Young's modulus in case of bidirectional fibre composites is equal to that obtained in longitudinal direction. The shear modulus is obtained using the following equation. For determination of Poisson's ratio (υ_{12}), a different set of specimens were used, along with a pair of strain gages bonded over the gage length of the sample in two mutually perpendicular directions. The strains were recorded simultaneously in longitudinal and transverse directions with the help of two strain indicators. The ratio of transverse to longitudinal strain directly gives the Poisson's ratio within the elastic range. The shear modulus (G_{12}) was determined similarly with 45˚ coupons using the following formula

$$G_{12} = \frac{1}{\frac{4}{E_s} - \frac{2(1-\upsilon_{12})}{E_{12}}} \quad (19)$$

Where, G_{12} is the shear modulus

E_s is the tensile modulus as obtained in 45˚ tensile tests

E_{12} is the tensile modulus as obtained in longitudinal direction

υ_{12} is the Poisson's ratio

A very minute variation was observed in the values of shear modulus and Poisson's ratio of various carbon fibre and hybrid laminates. Hence, a uniform value of G_{12} = 3.76 GPa, G_{23} = 3.5 GPa and $\nu_{12} = \nu_{23} = \nu_{31}$=0.3 has been considered.

The non-dimensional frequencies are calculated using the following formula:

$$\bar{\omega} = \omega a^2 \sqrt{\frac{\rho}{E_{11} h^2}}$$

where $\bar{\omega}$ is the non-dimensional frequency

ω is the natural frequency

ρ is the density of the plate

E_{11} is the tensile modulus as obtained in longitudinal direction

h is the thickness of the plate

Table 3 – Young's modulus for 8 layer laminated composite plates

Sl. No.	% of Carbon fiber	Lamination Sequence	Young's Modulus, E_{12} (GPa)
1	25	$[C\text{-}G\text{-}G\text{-}G]_s$	27.30
2	25	$[G\text{-}C\text{-}G\text{-}G]_s$	25.20
3	25	$[G\text{-}G\text{-}C\text{-}G]_s$	28.02
4	25	$[G\text{-}G\text{-}G\text{-}C]_s$	30.65
5	50	$[C\text{-}C\text{-}G\text{-}G]_s$	36.65
6	50	$[G\text{-}G\text{-}C\text{-}C]_s$	34.46
7	50	$[C\text{-}G\text{-}C\text{-}G]_2$	35.78
8	100	$[C\text{-}C\text{-}C\text{-}C]_s$	40.32

The present formulation is validated for vibration analysis of composites panels in free-free boundary conditions as shown in Table 4. The four lowest non-dimensional frequencies obtained by the present finite element are compared with numerical solution published by Ju *et al.* (1995).

Table 4 - Comparison of natural frequencies (Hz) from FEM with the frequencies for 8 layers for fully free boundary condition

Studies	Mode 1	Mode 2	Mode 3	Mode 4
Ju *et al*.(1995)	73.309	202.59	243.37	264.90
Present FEM	72.71	202.06	244.22	264.14

6.2 Modal Testing of Carbon fibre composite plates

1. Effect of number of layers for different boundary conditions

Modal frequencies obtained experimentally and those obtained from FEM analysis for the first four lowest frequencies for free-free boundary conditions are represented in Figure 7. The

experimental values are close to the values obtained from FEM analysis with a maximum deviation of 20%. It is observed from figure 10 that the modal frequencies increase with increase in the number of layers. The average increase in frequency is found to be 142 % and 279 % as the thickness increases from 4 layers to 8 and 12 layers respectively. The mode shapes for the first four frequencies obtained from ANSYS has been shown in figure 11.

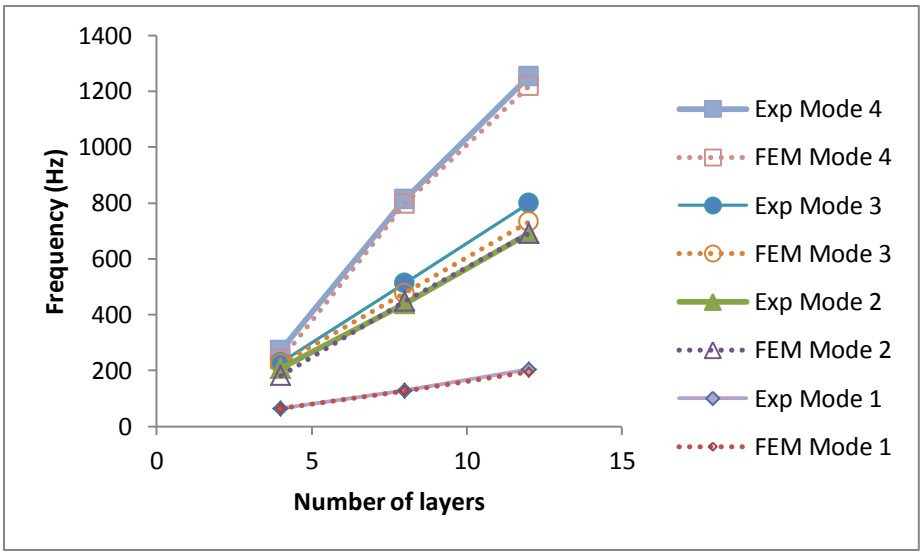

Figure 10 – Variation of natural frequency with number of layers for free-free support condition

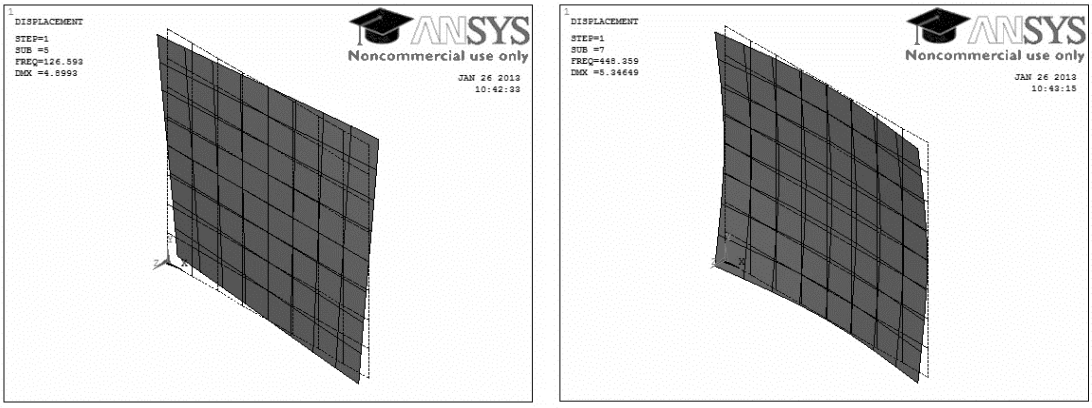

(a) (b)

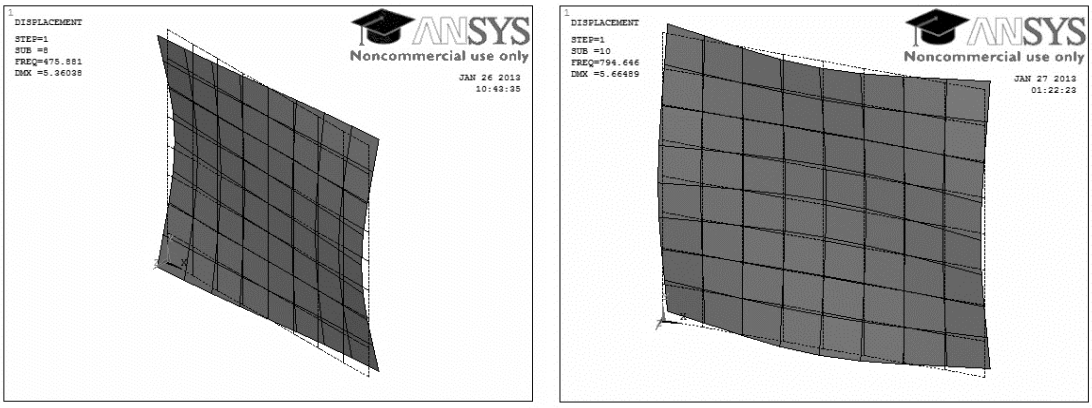

(c) (d)

Figure 11 - Mode shapes for first four modes for 8 layered CFRP plate for FFFF boundary condition: (a) 1st lowest frequency, (b) 2nd lowest frequency, (c) 3rd lowest frequency and (d) 4th lowest frequency.

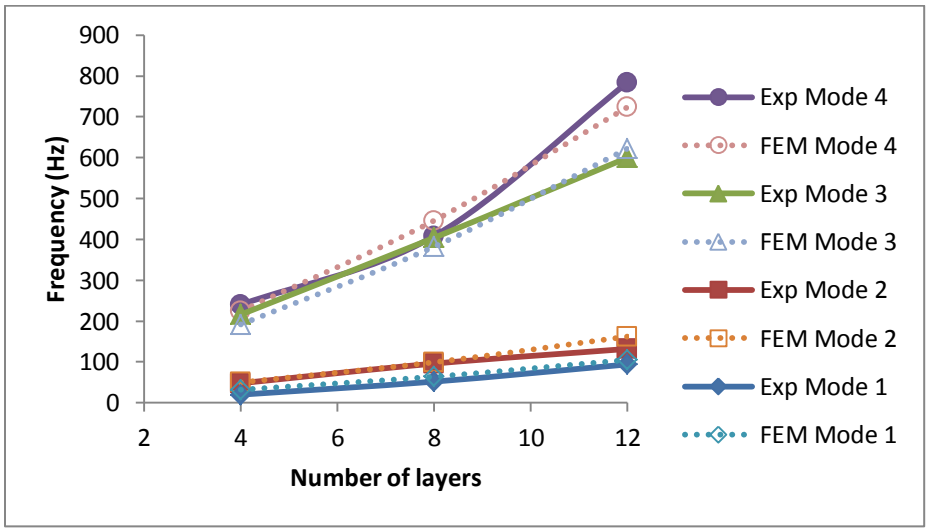

Figure 12 - Variation of natural frequency with number of layers for CFFF support condition

Figure 12 presents a graphical representation of the predicted as well as experimental results for CFFF support condition. The shape of the graph shows a marked similarity with the previous ones suggesting that the increase in thickness leads to an increase in stiffness which in turn is the reason for the increase in frequency. It is also observed that the frequencies in case of cantilever support are less than that of FFFF support condition. Another irregularity observed is the difference in values of 2nd and 3rd lowest frequencies which is found similar in the earlier case.

The mode shapes for the first four modes obtained from ANSYS has been shown in figure 13.

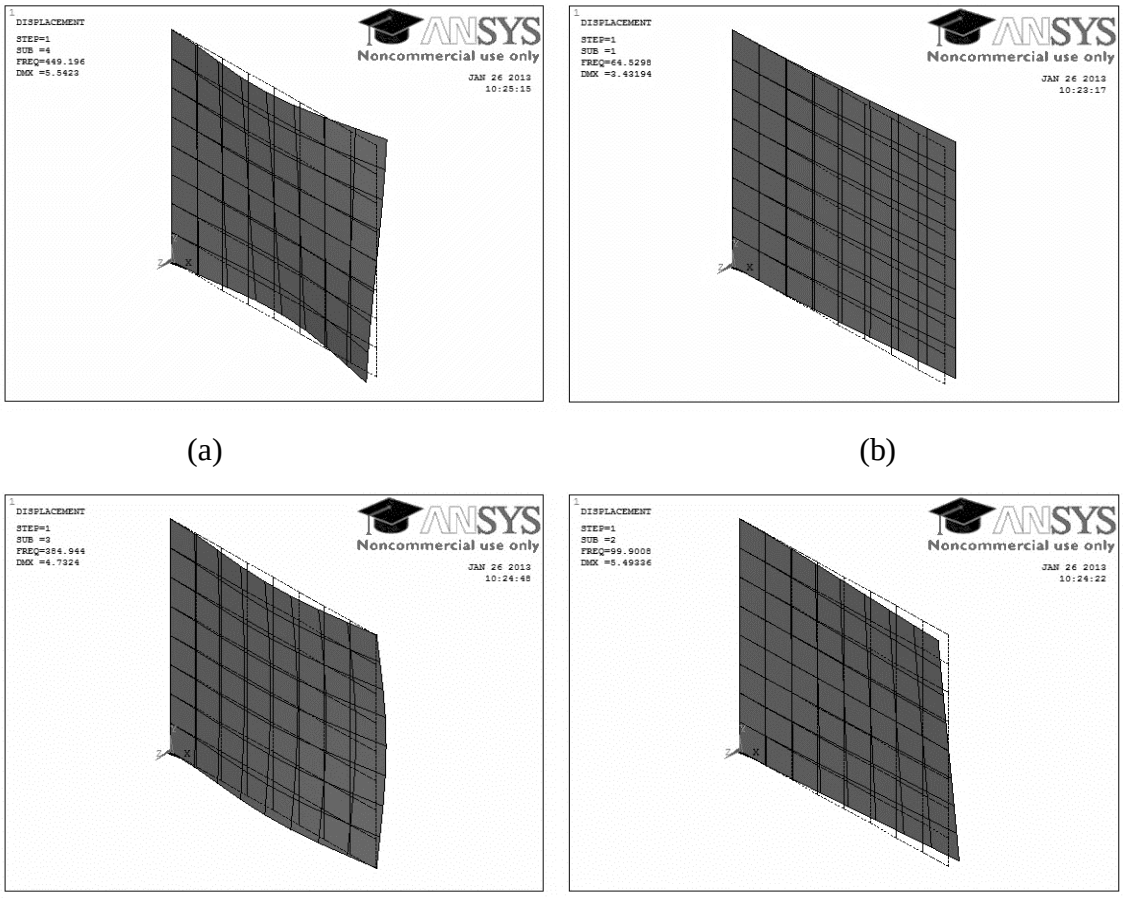

Figure 13 – Mode shapes for first four modes for 8 layered CFRP plate in CFFF boundary condition: (a) 1st mode, (b) 2nd mode, (c) 3rd mode and (d) 4th mode.

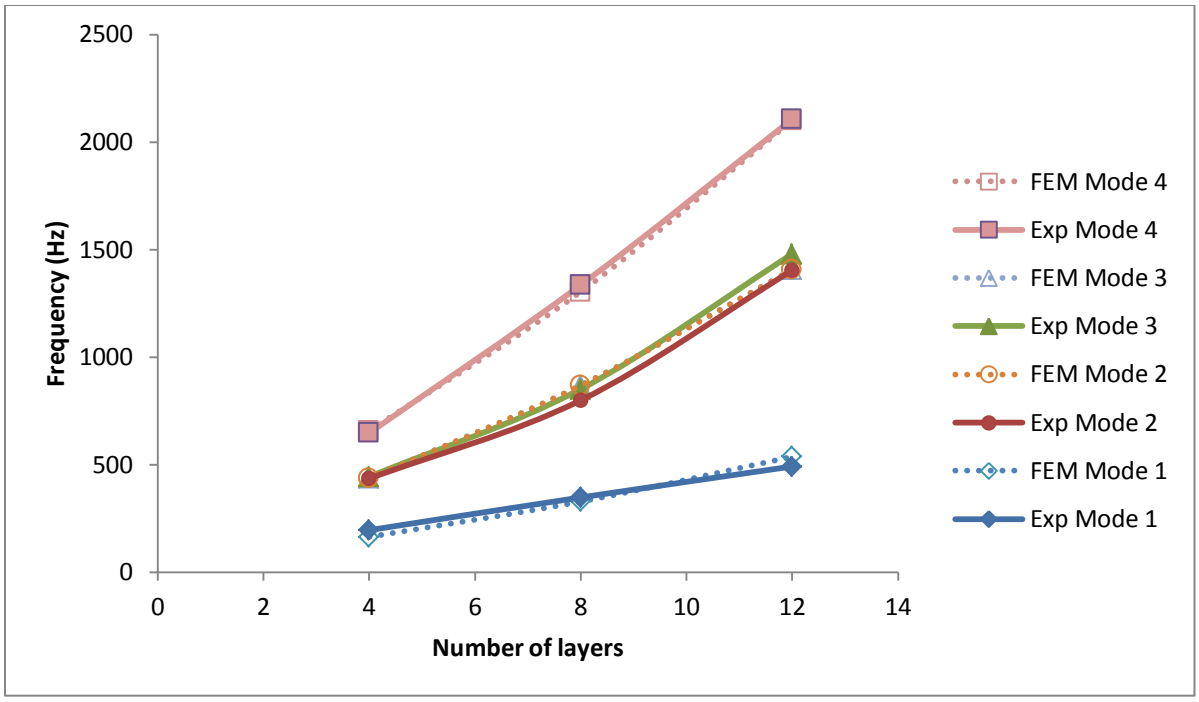

Figure 14 - Variation of natural frequency with number of layers for simply supported condition

Figure 14 presents a graphical representation of the predicted as well as experimental results for SSSS boundary condition. It is observed that the modal frequencies increase with the increase in number of layers. The average increase in frequency is found to be 90 % and 208 % as the thickness increases from 4 layers to 8 and 12 layers respectively. Figure 12 represents the mode shape for the first four modes as obtained from ANSYS 13.0. The 2nd and 3rd mode exhibit almost equal frequencies which can be accounted for by the similarity in the corresponding mode shapes in mutually perpendicular direction, as can be seen from figure 15 (b) and (c).

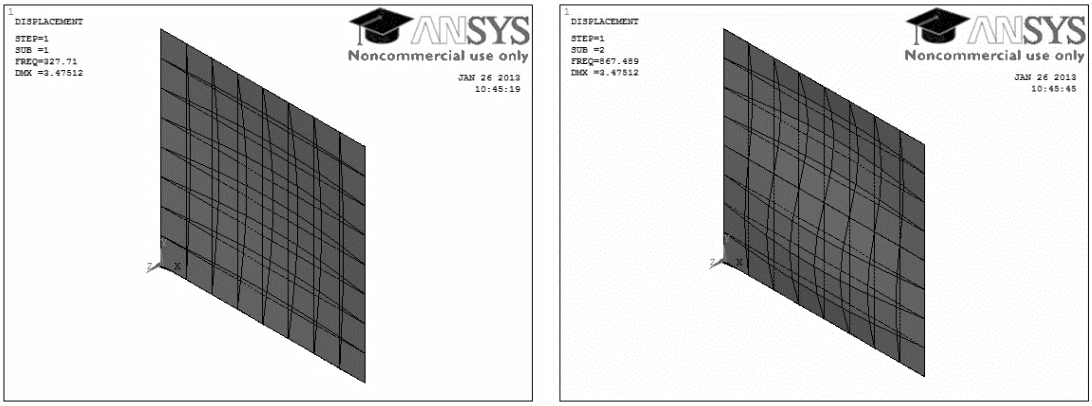

(a) (b)

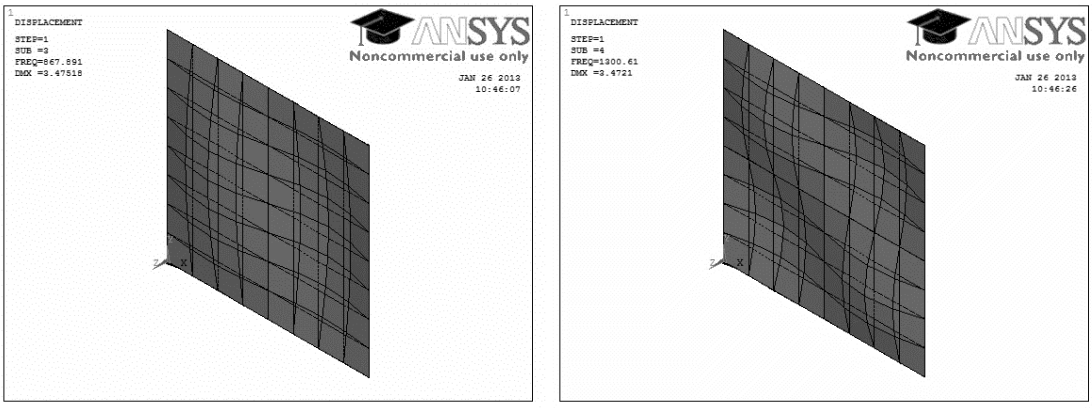

(c) (d)

Figure 15 – Mode shapes for first four modes for 8 layered CFRP plate for SSSS boundary condition: (a) 1st mode, (b) 2nd mode, (c) 3rd mode and (d) 4th mode.

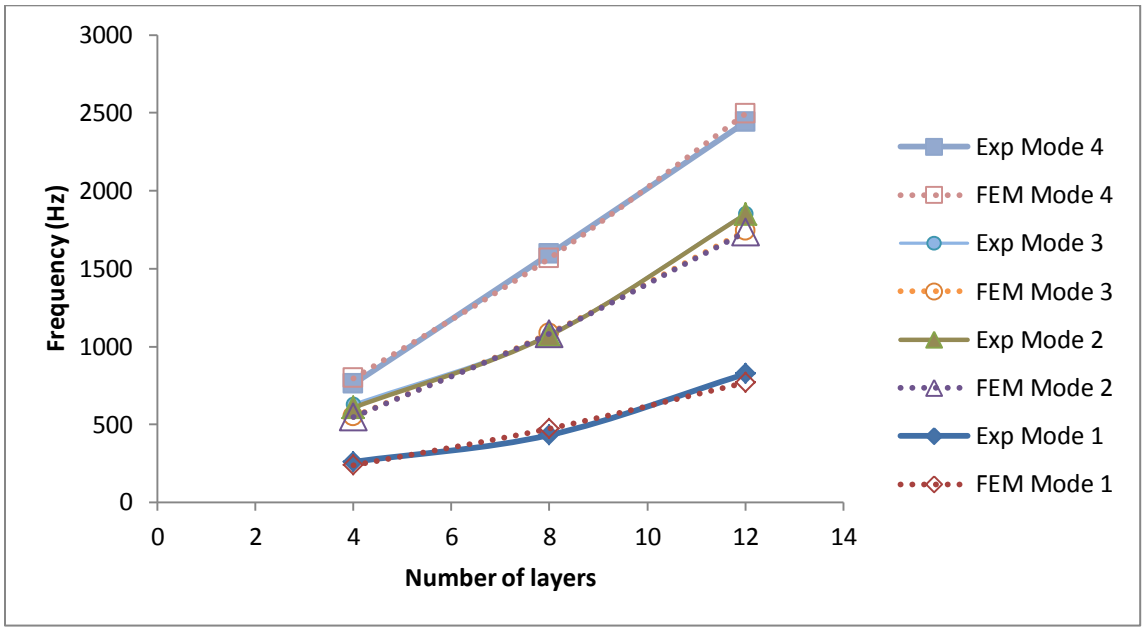

Figure 16 - Variation of natural frequency with number of layers for CSCS boundary condition

Figure 16 presents a graphical representation of the predicted as well as experimental results for CSCS boundary condition. There is an average increase of 80 % in the natural frequencies of vibration with increase in four layers. An average increase of 209 % is observed as the number of layers is increased from 4 to 12 layers. It can also be noted that the frequencies in this case are higher than simply supported conditions. Figure 17 shows the mode shapes for the corresponding frequencies as obtained from ANSYS 13.0.

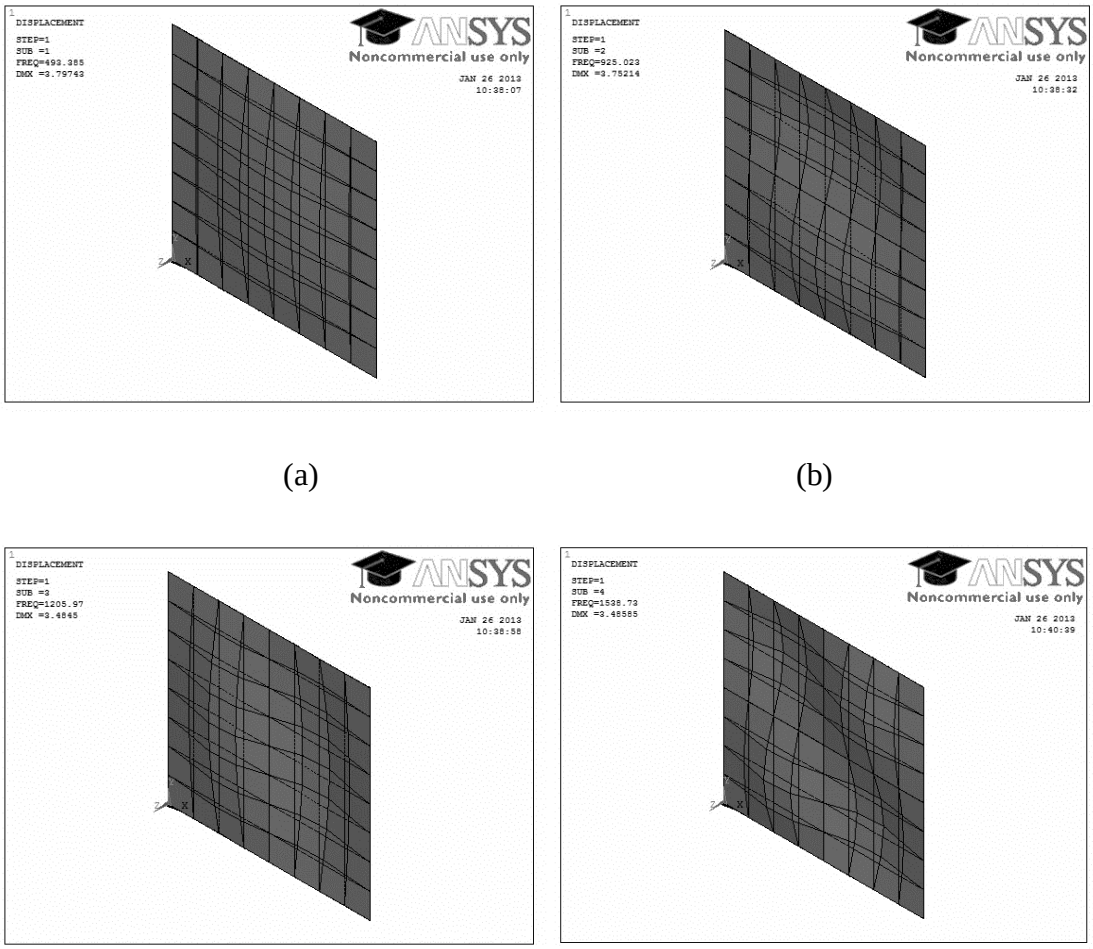

Figure 17 – Mode shapes for first four modes for 8 layered CFRP plate for CSCS boundary condition: (a) 1st mode, (b) 2nd mode, (c) 3rd mode and (d) 4th mode.

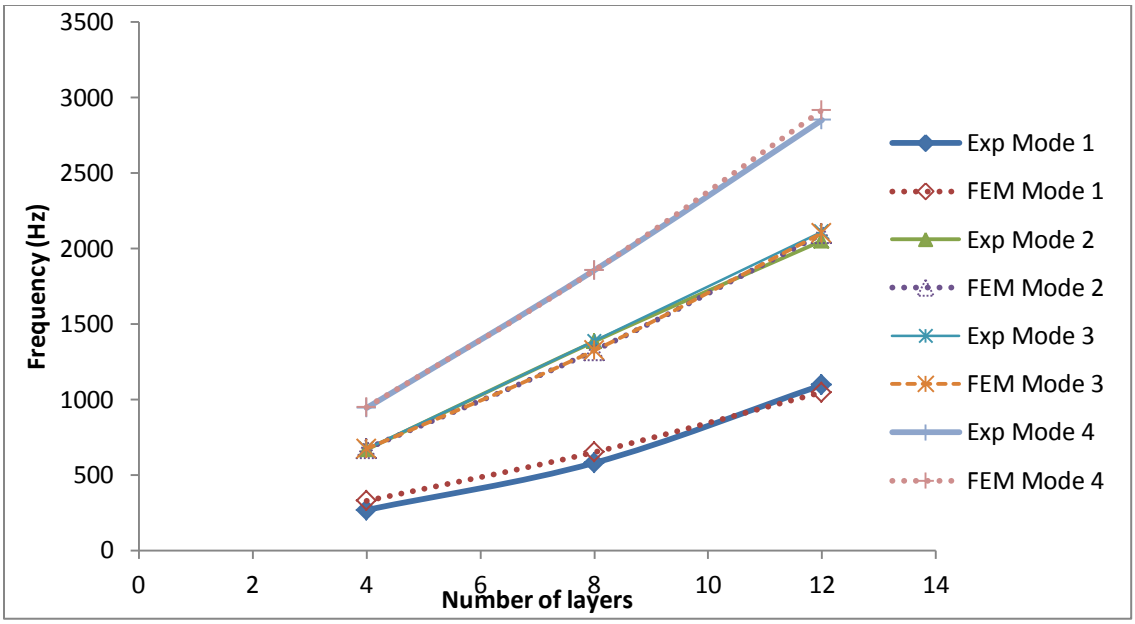

Figure 18 – Variation of natural frequency with number of layers for fully clamped support condition

A graphical representation of the predicted as well as experimental results for CCCC boundary condition represented by Figure 18 show same trend as observed in graph representing SSSS boundary condition. There is an average increase of 107 % in the natural frequencies of vibration with increase in four layers. An average increase of 187 % is observed as the number of layers is increased from 4 to 12 layers. The frequencies in case of CSCS boundary condition is found to be less than that of CCCC boundary condition and greater than that of SSSS boundary condition.

The corresponding mode shapes has been presented in Figure 19.

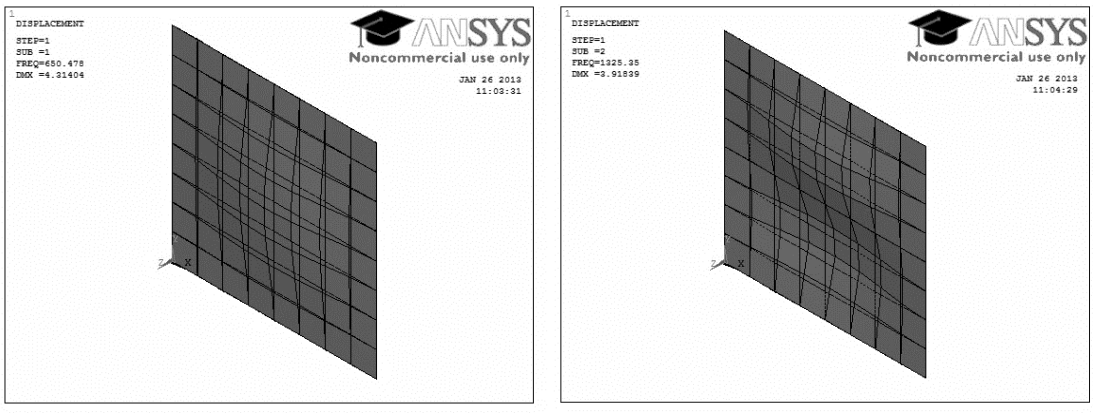

(a) (b)

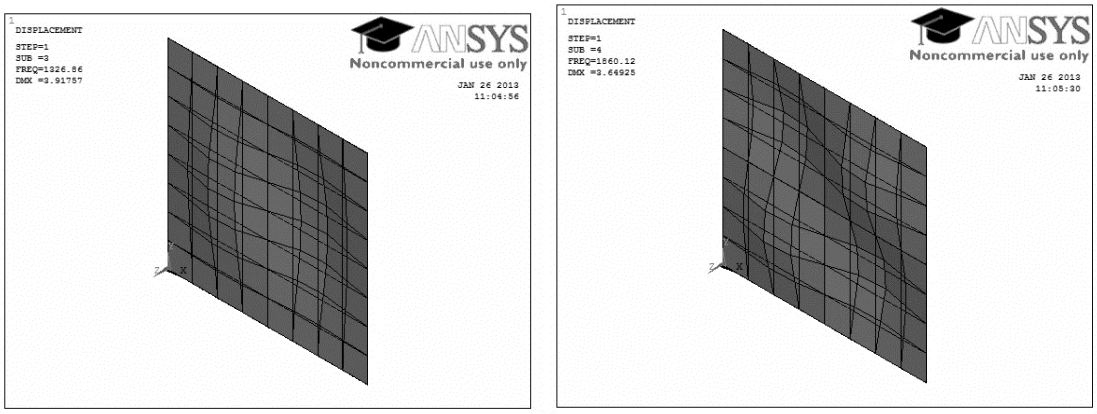

(c) (d)

Figure 19 – Mode shapes for first four modes for 8 layered CFRP plate for CCCC boundary condition: (a) 1st mode, (b) 2nd mode, (c) 3rd mode and (d) 4th mode.

2. Effect of boundary conditions

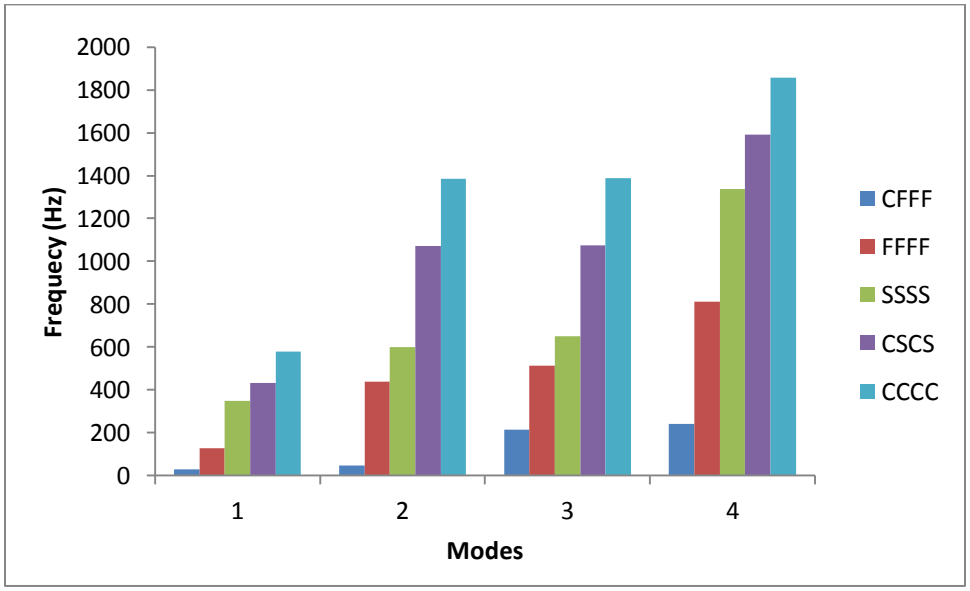

Figure 20 – Comparison of natural frequency of 8- layer CFRP plates for different boundary condition

Figure 20 gives a comparative representation of the frequencies for different modes for 8 layer laminated sheets for various boundary conditions. The frequencies for CCCC boundary condition are highest compared to all other boundary conditions. The frequencies are lowest in case of CFFF boundary condition. Fully clamped supports are more rigid and provide additional

constraint to rotation as compared to simply supported condition. We conclude that the stiffness of supports affect the frequencies directly. Increase in stiffness of supports leads to increase in modal frequencies.

3. Effect of aspect ratio

The variations in frequencies for different aspect ratio in fully free boundary condition are represented in Figure 21. The experimental and theoretical values can again be observed to be close. There is an increase in the frequencies with increase in the aspect ratio as observed in the figure. The mode shapes for corresponding of aspect ratio of 1, 2 and 4 are obtained from ANSYS 13.0 and are as shown in Figure 22-24.

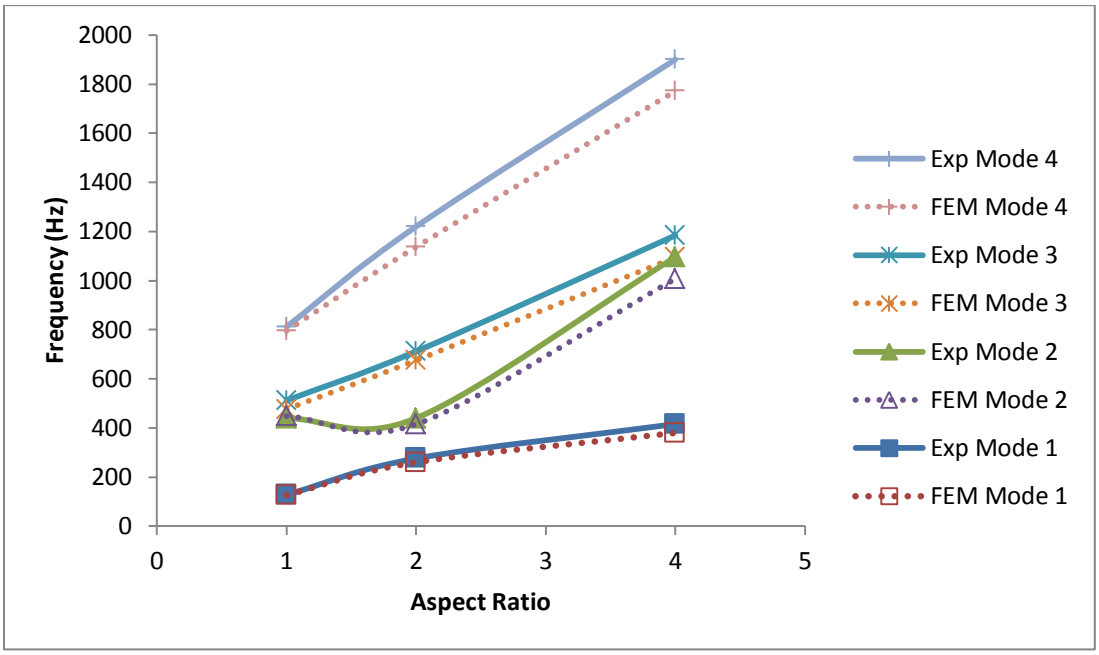

Figure 21 - Variation of natural frequency with aspect ratio for CFRP plates in FFFF boundary condition

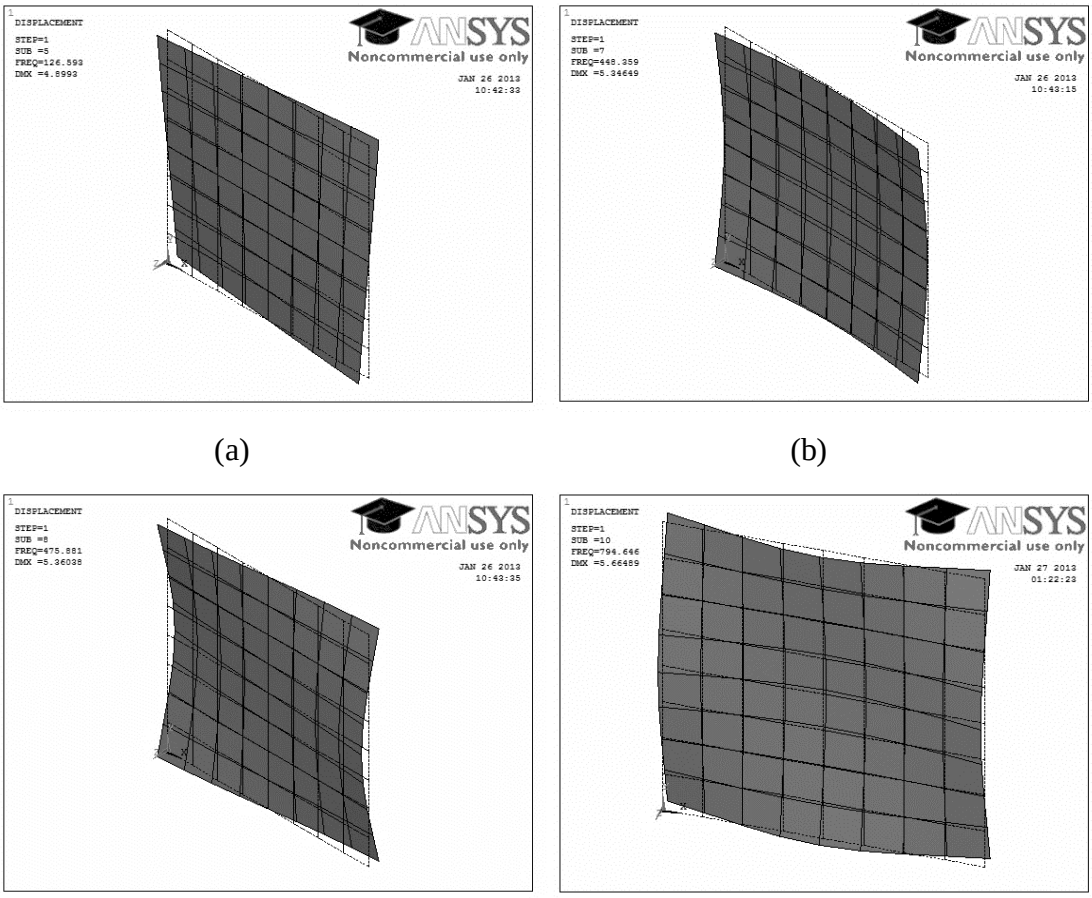

Figure 22 - Mode shapes for first four modes for 8 layered CFRP plate in FFFF boundary condition for aspect ratio 1 (a)1st lowest frequency, (b) 2nd lowest frequency, (c) 3rd lowest frequency, and (d) 4th lowest frequency.

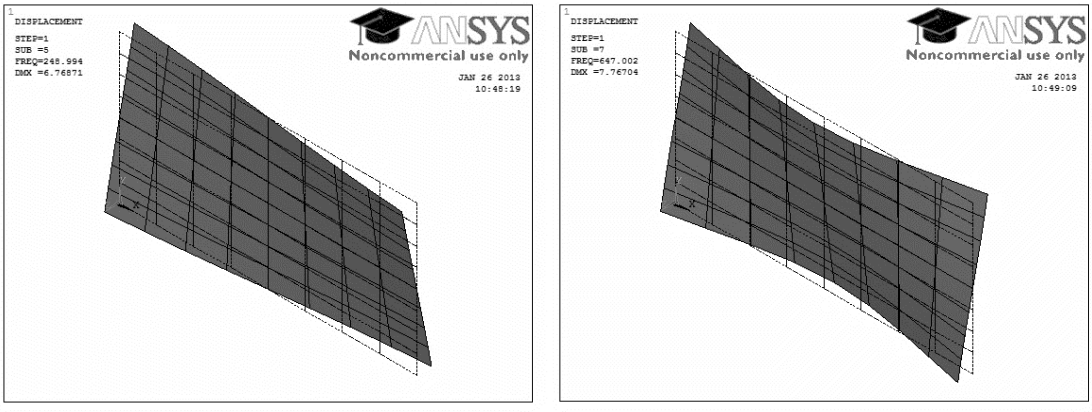

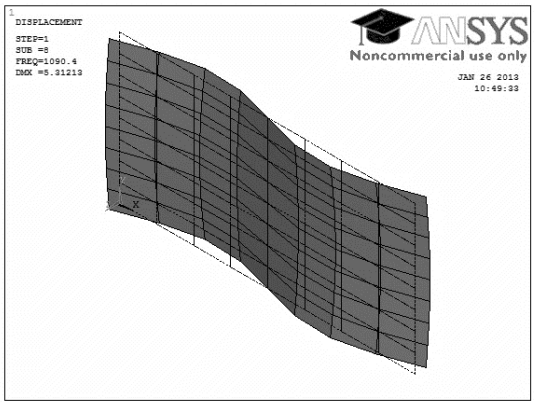

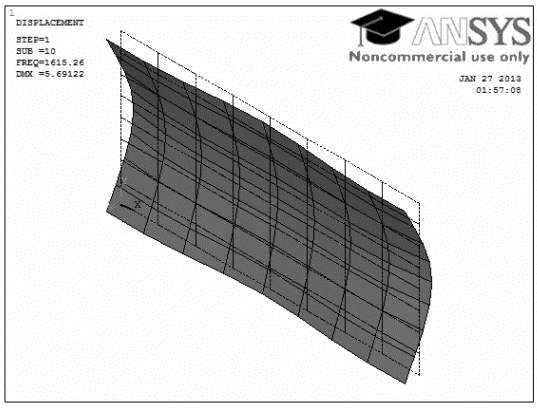

(c) (d)

Figure 23 - Mode shapes for first four modes for 8 layered CFRP plate in FFFF boundary condition for aspect ratio 2 (a) 1st lowest frequency, (b) 2nd lowest frequency, (c) 3rd lowest frequency, and (d) 4th lowest frequency.

.

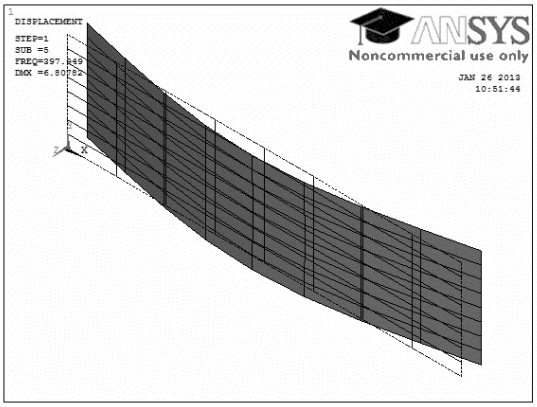

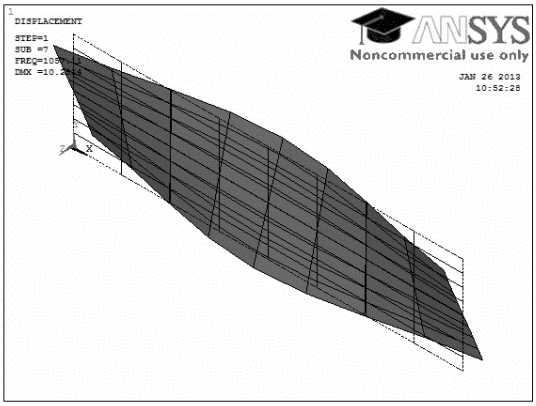

(a) (b)

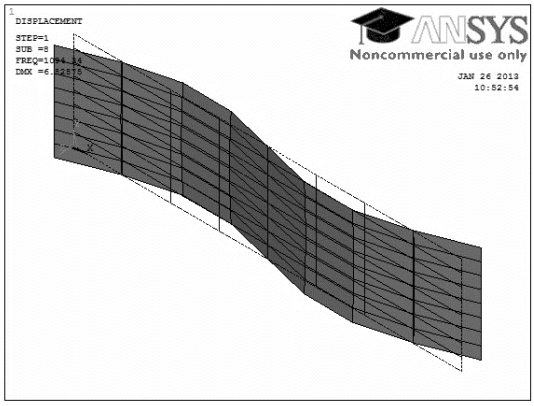

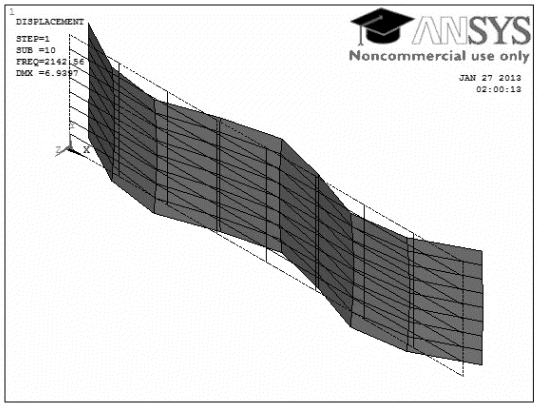

(c) (d)

Figure 24 - Mode shapes for first four modes for 8 layered CFRP plate in FFFF boundary condition for aspect ratio 4: (a)1st lowest frequency, (b) 2nd lowest frequency, (c) 3rd lowest frequency, and (d) 4th lowest frequency.

4. Effect of size of plates

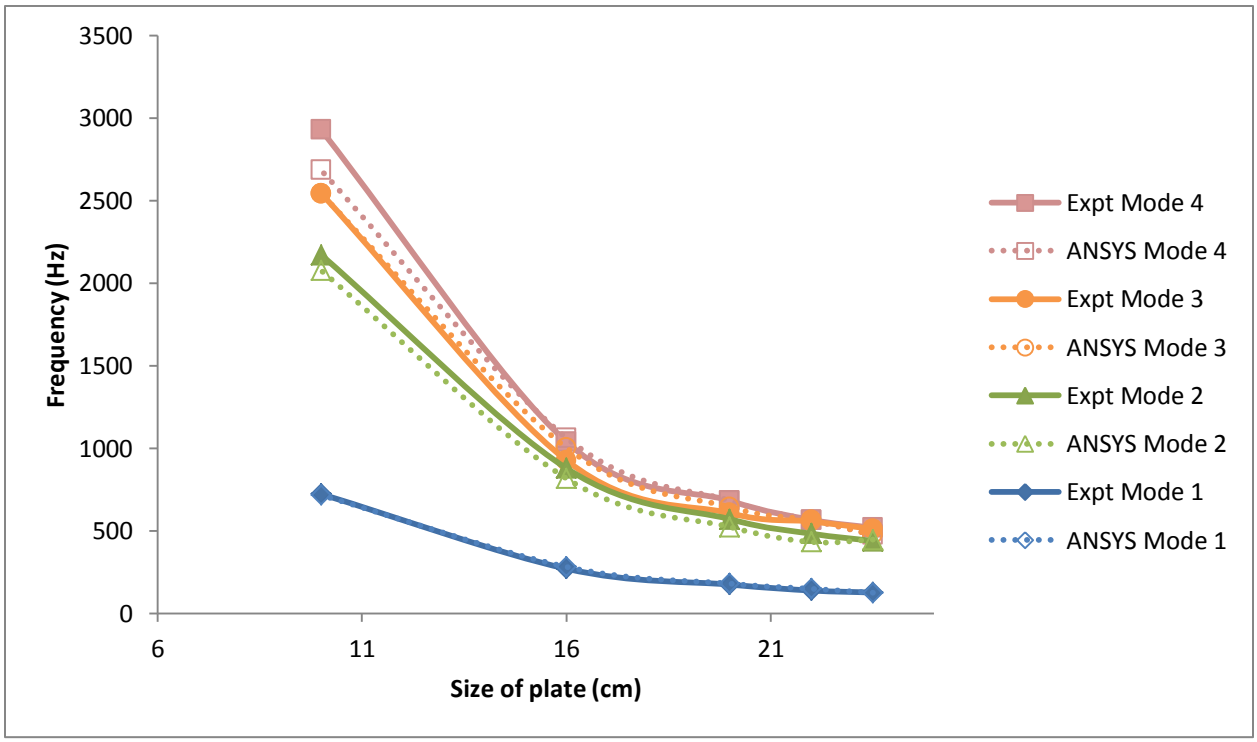

Figure 25 – Effect of size on the natural frequency of CFRP plates in FFFF boundary condition

The effect of size of square plates on the natural frequency of CFRP plates is shown in Figure 25. From the figure it is observed that with increase in size the natural frequencies decrease. It is also observed that variation is more predominant in higher modes. It is seen that the frequencies increase approximately by 75.5 % as the size of the square plate is doubled from 10 cm to 20 cm. The variation in natural frequency is 62% when the size increases from 10 cm to 16 cm and 35 % when size increases from 16 cm to 20 cm. Further when the size is increased to 22 cm there is 18% increase in the frequency showing that at greater sizes the effect of size on the natural frequency reduces.

5. Effect of temperature conditioning.

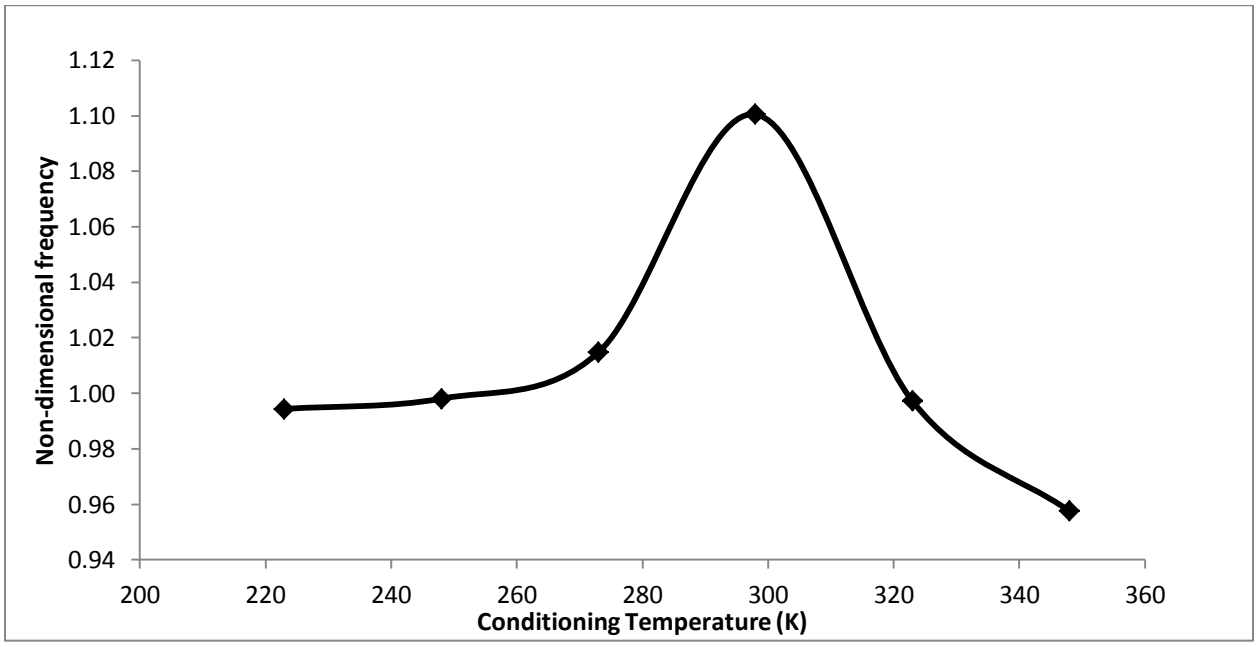

Figure 26 – Effect of heating and cooling (flight condition) on non-dimensional frequencies of CFRP plates

To study the effect of temperature conditioning the specimen is heated at a certain temperature and then cooled up to room temperature. This represents the after flight ground condition of the aircrafts. This differs from the inflight condition in a way that the testing is done at room temperature after temperature conditioning for particular time duration. There is a decrease in the stiffness and frequency with deviation of conditioning temperature from the manufacturing temperature as evident from figure 26. This variation in the stiffness can be attributed to the development and release of complex residual stresses due to volume changes in the matrix, change in microstructure and development of hygrothermal stresses. In case of bidirectional fibres, the change in natural frequencies along both the directions is less compared to that in unidirectional fibres whose transverse properties are dominated by the matrix characteristics. The coefficient of thermal expansion is greater for matrix in comparison to the fibre. The fundamental frequency is affected the most, up to 10 %. Since the percentage of variation of natural frequencies is less than 10 % it can be concluded that thermal treatment does not produce any pronounced variation in the stiffness of the composites.

6. Effect of hygrothermal conditions

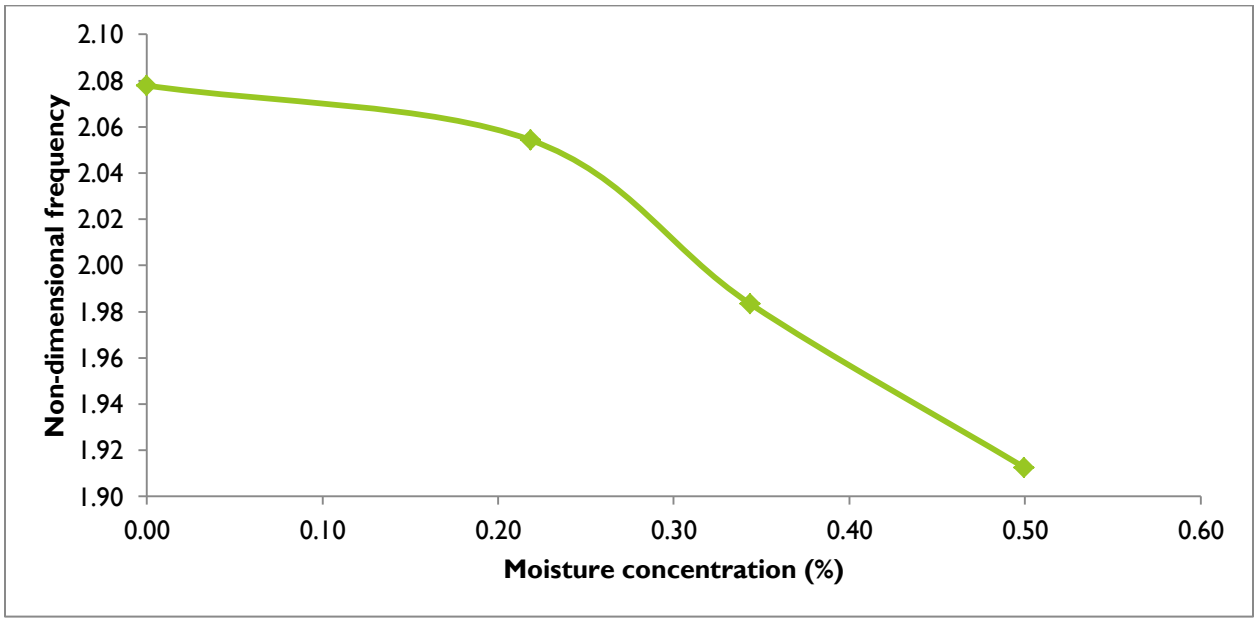

Figure 27 – Variation of non-dimensional frequencies of CFRP plates with moisture concentration

With increase in moisture concentration the modal frequencies of CFRP plates is observed to decrease as seen in Figure 27. This increase can be attributed to the development of Regardless of the application, once cracks have formed within polymeric materials, the integrity of structure is significantly compromised. Microcracking induced by environment is a long-standing problem in polymer composites.

The amount of moisture absorbed by the epoxy matrix is significantly greater than that by the reinforcement carbon fibers. This results in a mismatch in the moisture-induced volumetric expansion between the fiber and polymer matrix. That leads to the evolution of localized stress and strain fields in the composite. The moisture absorption most often leads to changes in the thermophysical, mechanical and chemical characteristics of the epoxy matrix by plasticization and hydrolysis. Integrity of polymer composites in terms of matrix cracking and/or fiber/matrix debonding/discontinuity by humid ageing may be reflected by moisture absorption.

7. Effect of repeated thermal loading

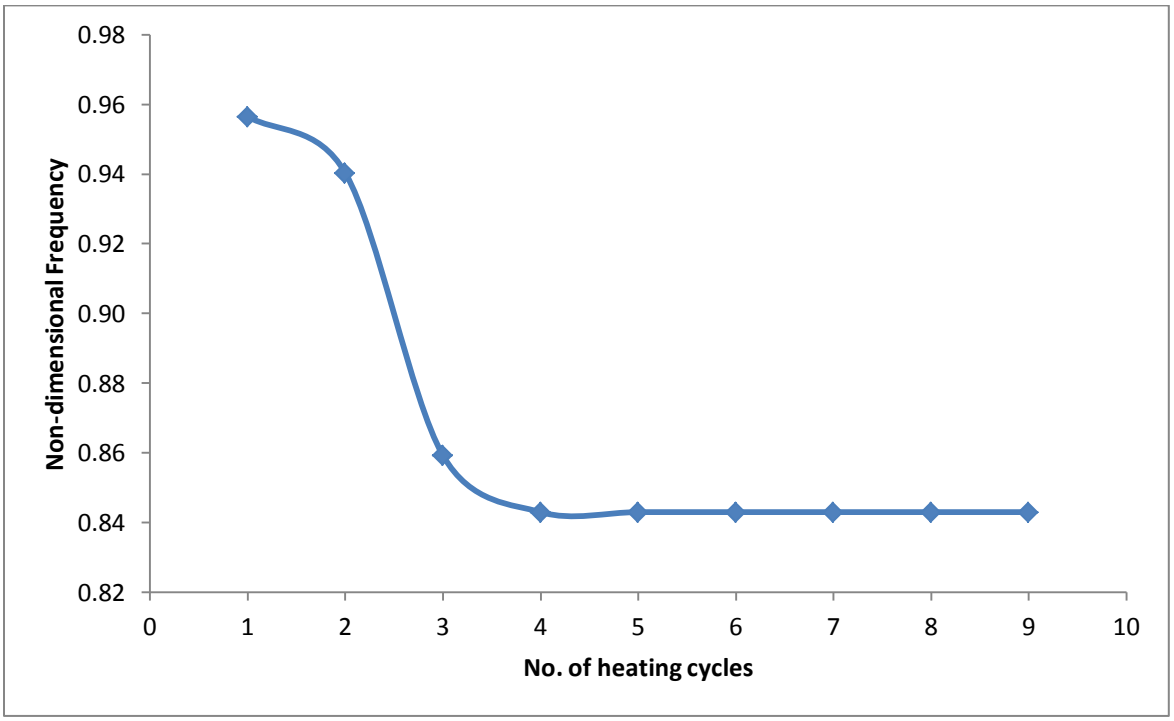

Figure 28 – Variation of non-dimensional frequency with the number of heating cycles

The carbon composite laminate was heated upto 348 K and cooled to room temperature before testing. The non-dimensional frequencies obtained from the free vibration analysis have been represented in figure 28. Repeated cycles of heating and cooling cause degradation of the laminates. It has been observed that the modal frequencies attain a constant value after decreasing for the first two cycles. The value remains unchanged for 30 test cycles when subjected to conditioning temperature. Jones (1975) showed that degradation of the material occurs after 10^6 cycles of heating and cooling.

These frequencies should be used for all practical design purposes and every structure is to be temperature conditioned to maximum possible working temperature for a certain minimum number of cycles before being put to industrial use.

8. Effects of type of fibre

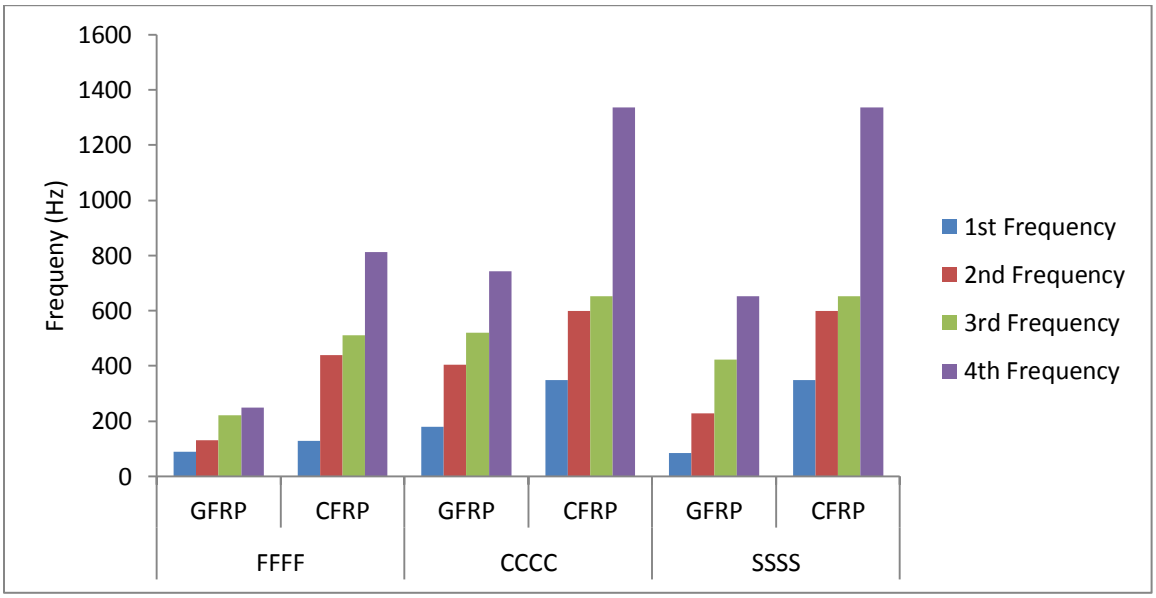

Figure 29 - Variation of natural frequency with type of fibre

Figure 29 shows that the frequencies of vibration of CFRP plates is significantly higher than the values obtained for GFRP as presented by Basa and Dwibedi (2012) for the same size of the plate and boundary condition. The strength and stiffness of carbon fibre composites is inherently greater than that of glass fibre composite. From the tensile tests conducted it was observed that the Young's Modulus for CFRP plates is 40.32 GPa and GFRP plates is 7.0 GPa. CFRP laminates undergo brittle failure whereas GFRP plates exhibit ductile behaviour before failure.

6.3 Buckling characteristics of composite laminates

The buckling loads were found experimentally and analytically for square composite laminates in CFCF boundary condition. The analytical values were found to be in good agreement with the experimental values. From the results obtained it was observed that buckling loads increased with increase in the number of layers of carbon fibre in CFRP plates, as can be seen in figure 30. This can attributed to bending, stretching and coupling effects in composite laminates.

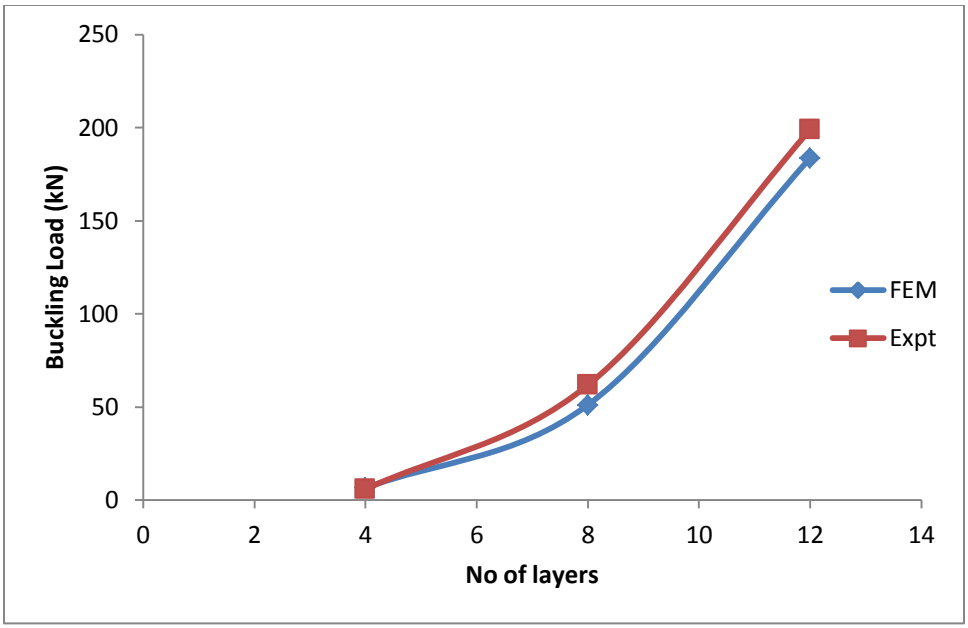

Figure 30 – Variation of buckling load with number of layers of carbon fibre in CFRP plates in CFCF boundary condition

6.4 Glass-Carbon/epoxy hybrid composite plates

The variation of frequency of vibration of 8 layered carbon/glass hybrid plates with 25 % carbon and 75 % glass reinforcement has been shown in figure 31. The sequence of carbon fibre in the composite shown in above figure as 1-8, 2-7, 3-6 and 4-5 represent $(C\text{-}G\text{-}G\text{-}G)_s$, $(G\text{-}C\text{-}G\text{-}G)_s$, $(G\text{-}G\text{-}C\text{-}G)_s$ and $(G\text{-}G\text{-}G\text{-}C)_s$ respectively. The natural frequency is lowest for $(G\text{-}C\text{-}G\text{-}G)_s$ sequence for all the modes. In case of hybrid composites, the failure was initially observed to be due to delamination between layers of two different fibres. This can be attributed to the weak bonding between the glass and carbon fibres. Since in the case of $(C\text{-}G\text{-}G\text{-}G)_s$ carbon fibres form the outermost layer, they provide more strength compared to $(G\text{-}C\text{-}G\text{-}G)_s$ and almost equal to $(G\text{-}G\text{-}C\text{-}G)_s$ where two glass fibres provide strength equivalent to one layer of carbon fibre. In $(G\text{-}G\text{-}G\text{-}C)_s$, the presence of carbon in the core is results in higher strength because of its greater stiffness. The ultimate tensile stresses of the hybrid laminates during the tensile testing showed a similar trend.

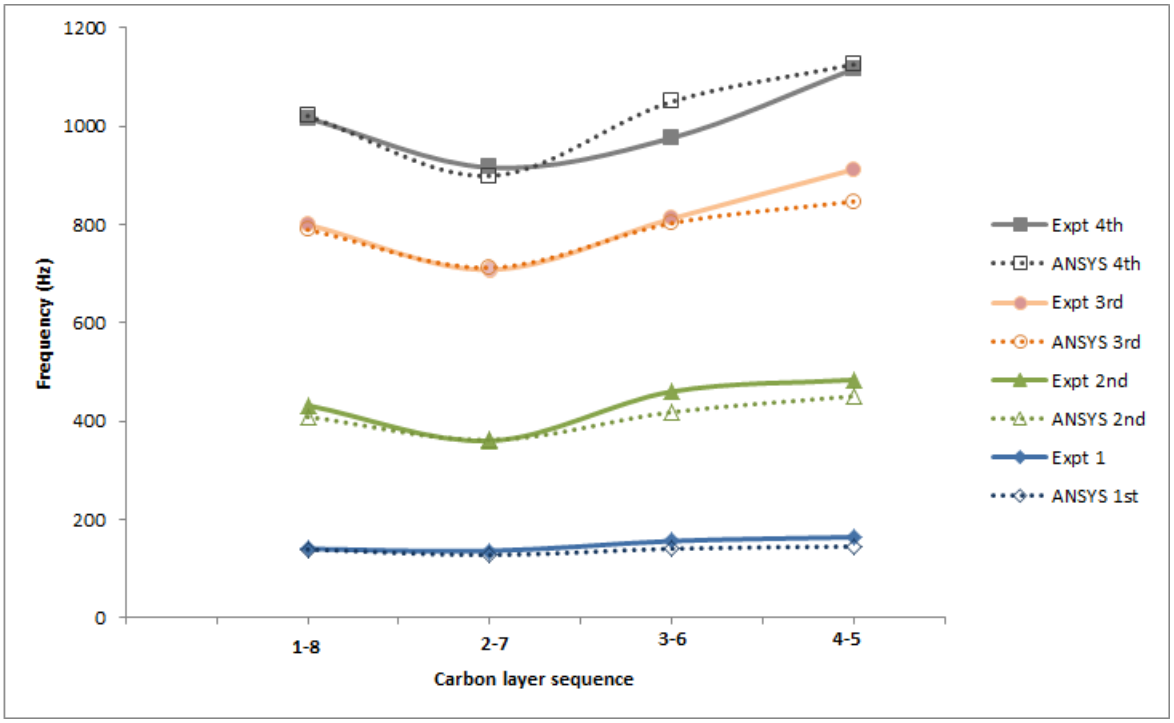

Figure 31 – Variation in natural frequency with the stacking sequence of carbon fibre in carbon/glass hybrid plates with 25 % carbon fibre

The variation of frequency of vibration of 8 layered carbon/glass hybrid plates with 50% carbon and 50% glass reinforcement for stacking sequence (C-C-G-G)s, $(C\text{-}G\text{-}C\text{-}G)_2$ and (G-G-C-C)s has been shown in Figure 32. It is observed that the natural frequency for (C-C-G-G)s is highest owing to the greater stiffness of the laminated plates with glass core. The frequency was observed to be the least for plates with alternate layers of carbon/glass fibre stacking. This can be attributed to the lower stiffness due to greater tendency to debond at interface between glass and carbon fibre which is highest in this case.

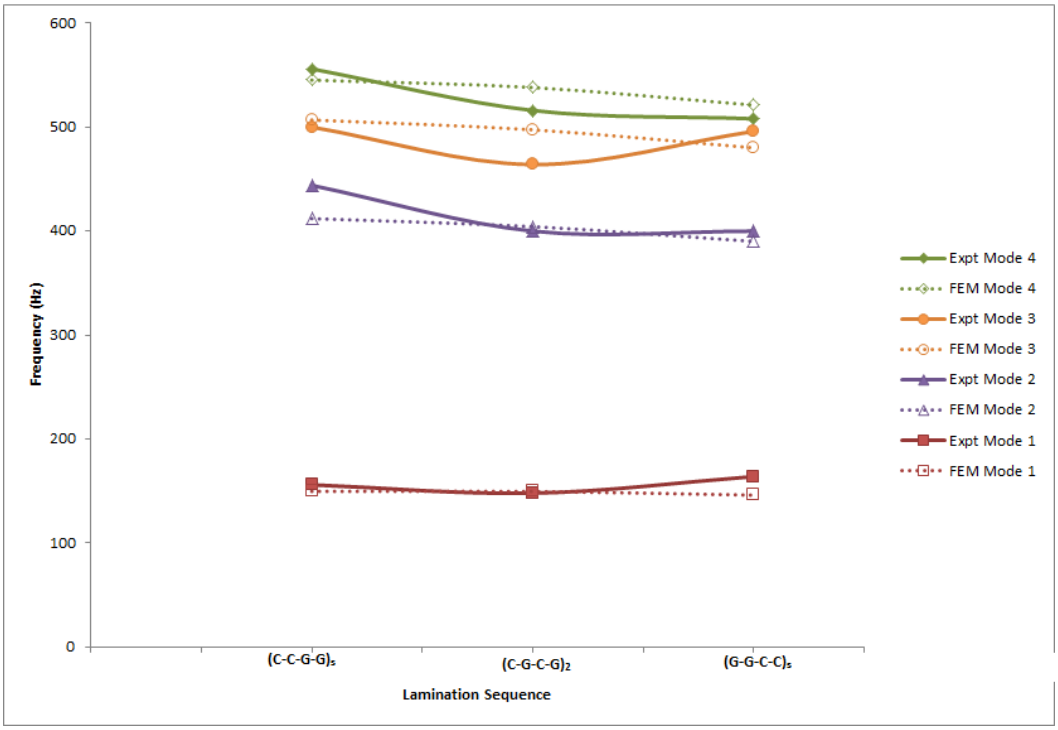

Figure 32 - Variation in natural frequency with the stacking sequence of carbon fibre in carbon/glass hybrid plates with 50 % carbon fibre

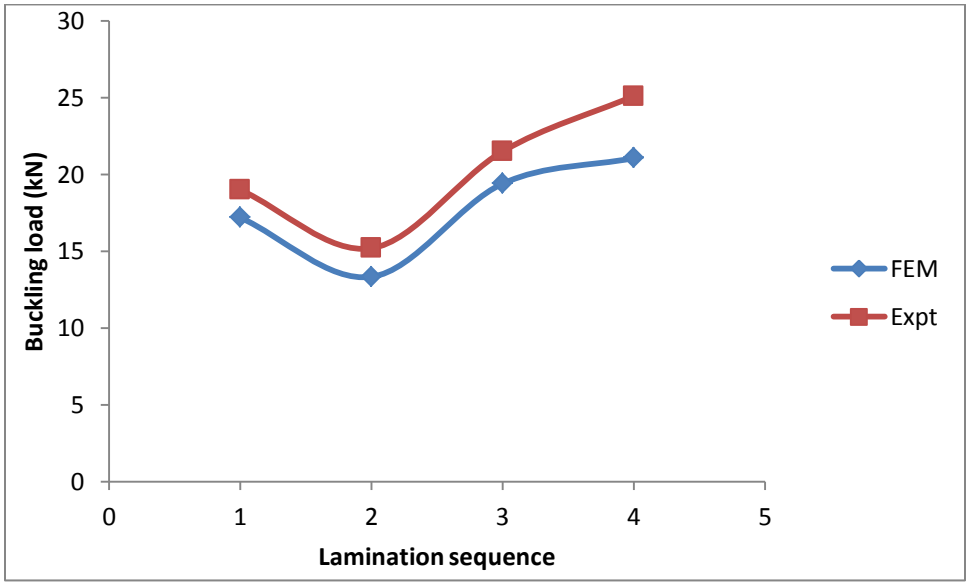

Figure 33 - Variation of buckling load with lamination sequence of CFRP plates in CFCF boundary condition with 25 % carbon fibre

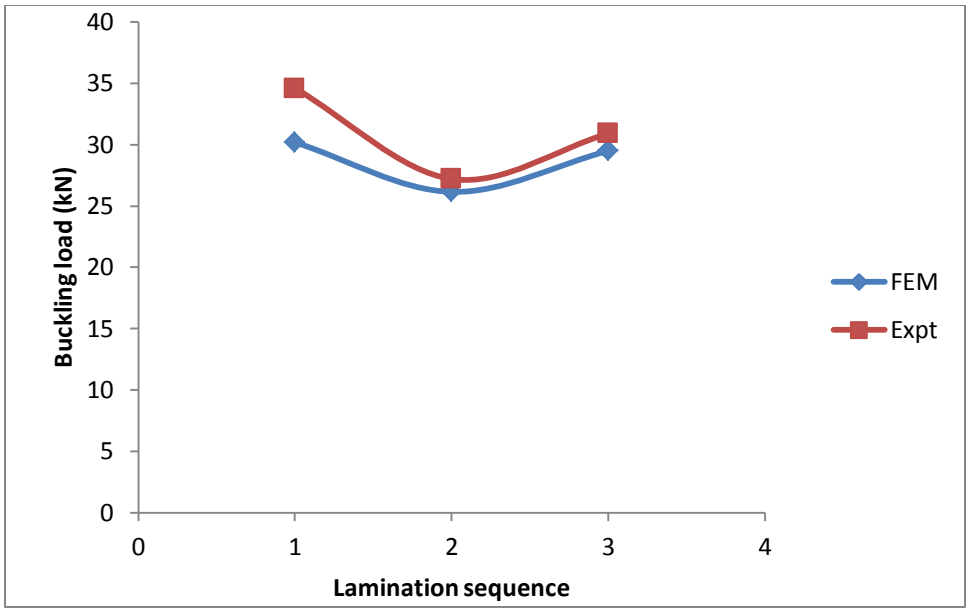

Figure 34 - Variation of buckling load with lamination sequence of CFRP plates in CFCF boundary condition with 50 % carbon fibre

Buckling analysis was also performed on glass-carbon/epoxy laminates previously tested for free vibration analysis to study the effect of different percentage composition and lamination sequence of carbon and glass fibre. It was observed that the buckling loads for glass-carbon/epoxy hybrid laminates follow a different trend from that observed in case of vibration analysis conducted. In this case the plies possessing higher modulus of elasticity when present on the outermost layer, gives maximum buckling load as can be seen from the figures 33 and 34. A sudden decrease in buckling load is observed when a single glass fibre is present as the outermost layer. This gradually increases with increase in the number of glass fibre layers in the exterior plies.

CHAPTER - 7

CONCLUSION

The present work deals with the study of vibration and buckling characteristics of laminated composite plates. Experimental studies were conducted for determination of natural frequencies of carbon/epoxy composite laminates. Free vibration analysis of laminated composite plates was done using FFT analyzer by varying various parameters. The obtained results were validated and the mode shapes for various modes of vibration were determined using finite element package, ANSYS 13.0. The critical buckling load was determined for the laminates. A special case of hybrid laminates was studied to understand the effect of lamination sequence on the vibration and buckling characteristics of carbon-glass/epoxy composite plates.

Results are presented for the vibration and buckling characteristics of carbon/epoxy composites plates and carbon-glass/epoxy laminates. The effects of various geometrical parameters like size, aspect ratio, and boundary conditions on the natural frequencies of vibration has been analysed. The effects of temperature and moisture conditioning on the vibration characteristics of CFRP plates are also studied. Results for fatigue testing have also been presented.
The conclusions are presented separately for three cases.

1. Vibration of laminated carbon composite plates

The natural frequencies of carbon composite plates have been reported for simply supported, fully clamped, cantilever, free-free and CSCS boundary conditions. The effect of temperature and moisture concentration was also studied. From the experiments it was observed that

- The frequency of vibration of composite plates increase with increase in the number of layers of fiber for all the support conditions.
- The frequency of vibration was noted to be highest for fully clamped condition and lowest for cantilever boundary condition which can be attributed to the increased stiffness

of supports. When compared with the results reported for GFRP, it was observed that the modal frequencies for CFRP were considerably higher than that of GFRP accounting for its better performance.

- The modal frequencies are also observed to increase with the increase in the aspect ratio. Smaller sized specimens show higher frequencies and the effect of size is more predominant in higher modes.
- Thermal treatment representative of after flight conditions on CFRP laminates leads to decrease in frequency when subjected to temperatures either higher or lower than manufacture temperature.
- However, in case of cryogenic temperatures the decrease is not uniform. A sudden decrease is observed at 273 K after which a small rise in frequency is observed.

2. Buckling analysis of laminated carbon composite plates

The buckling loads were found experimentally and analytically for square composite laminates in CFCF boundary condition.

- It was observed that buckling loads increased with increase in the number of layers of carbon fibre in CFRP plates.

3. Glass-Carbon/epoxy hybrid composite plates

- In case of hybrid plates, the frequencies are observed to change with the stacking sequence. For hybrids with 25% laminate layers of carbon fibre and the rest 75% glass fibre, the minimum frequency is observed in case of $(G\text{-}C\text{-}G\text{-}G)_s$ sequence and for hybrids with 50% carbon fibre laminates, the minimum frequency is observed for $(C\text{-}G\text{-}C\text{-}G)_2$ sequence.
- Plies possessing higher modulus of elasticity when present on the outermost layer, gives maximum buckling load.
- The effectiveness of hybridisation increases if materials with high values of young's modulus form the outermost layer.
- The buckling loads of hybrid laminates with same mass and small amount of fibre with high-stiffness are higher than those corresponding to homogeneous laminates. In this way, the fabrication of hybrid laminates enables to optimize the structural response to

external loads. Thus, composite structures can be designed for optimal structural, technological and economic response for a given geometry and state of stress of structural elements.

CHAPTER - 8

FUTURE SCOPE

The present study can be extended to the following areas:

- Study of hygrothermal effects on vibration characteristics of carbon-glass hybrid laminates
- Study of hygrothermal effects on buckling characteristics of carbon composite plates and carbon-glass hybrid laminates
- Vibration and buckling tests to study the effectiveness of hybridization using different combinations of constituent fibers
- Effect of joints on vibration and buckling studies of composite laminates
- Develop computer program for optimal design of composite structures by using the data obtained from the present study

CHAPTER - 9

LIST OF PUBLICATIONS

1. Meher, S., Nayak, N. and Sahu, S.K., Modal Analysis of Woven Fiber Composite Plates for different Aspect Ratios, Indian Society for Non-Destructive Testing - NDE 2012, New Delhi, 8-10 December, 2012
2. Nayak, N., Meher, S. and Sahu, S.K., Vibration Measurement of Woven Fiber Laminated Composite Plates, Indian Society for Non-Destructive Testing - NDE 2012, New Delhi, 8-10 December, 2012
3. Meher, S., Nayak, N. and Sahu, S.K., Experimental and numerical study on vibration of woven fiber carbon/epoxy laminated composite plates, ICMAT 2013, Singapore (accepted for presentation)

CHAPTER - 10

REFERENCES

1. Aiello, M.A. and Ombres, L. (1997): Maximum buckling loads for unsymmetric thin hybrid laminates under in-plane and shear forces, *Composite Structures*, 36, 1-11.
2. ANSYS user's manual (2010): *Sawnson Analysis Systems Inc*.
3. ASTM Standard: D 3039/D 3039M-08 (2008): Standard test method for tensile properties of polymer matrix composite materials.
4. ASTM Standard: D 5229/D 5229M-04 (2004): Standard test method for moisture absorption.
5. ASTM Standard: D 5687/D 5687M-07(2007): Standard guide for preparation of flat composite panels with processing guidelines for specimen preparation.
6. Aydogdu, N. and Timarci, T. (2003): Vibration analysis of cross ply laminated square plate with general boundary conditions, *Composite Science and Technology*, 63, 1061-1070.
7. Badie, M.A., Mahdi, E. and Hamouda, A.M.S. (2011): An investigation into hybrid carbon/glass fiber reinforced epoxy composite automotive drive shaft, *Materials and Design*, 32, 1485-1500.
8. Barai, A. and Durvasula, S. (1992): Vibration and buckling of hybrid laminated curved panels, *Composites*, 21, 15-27.
9. Basa, D. and Dwibedi, S. (2012): Effects of cut-out on natural frequency of glass fibre-epoxy composite plates, Department of Civil Engineering, National Institute of Technology, Rourkela.
10. Botelho, E.C., Pardini, L.C. and Rezende, M.C. (2005): Hygrothermal effects on damping behaviour of metal/glass fiber/ epoxy hybrid composites, *Materials Science and Engineering A*, 399, 190-198.
11. Bruno, D. and Lato, S. (1991): Buckling of moderately thick composite plates, *Composite Structures*, 18, 65-75.
12. Bunsell, A.R. and Harris, B. (1974): Hybrid carbon and glass fibre composites, *Composites*, 157-164.

13. Cawley, P. and Adams, R. D. (1978): The predicted and experimental natural modes of free-free CFRP plates, *Journal of Composite Materials*, 12, 336-347.
14. Cawley, P. and Adams, R. D. (1979): A Vibration Technique for Non-Destructive Testing of Fibre Composite Structures, *Journal of Composite Materials*, 13, 161-175.
15. Chai, G. B. (1994): Free vibration of generally laminated composite plates with various edge support conditions, *Composite Structures*, 29, 249-258.
16. Chai, G.B., Chin, S. S., Lim, T. M. and Hoon, K. H. (1993): Vibration analysis of laminated composite plates: TV-holography and finite element method, *Composite Structures*, 23, 273-283.
17. Chai, G. B. and Hoon, K. H. (1992): Buckling of generally laminated composite plates, *Composites Science and Technology*, 45, 125-133.
18. Chai, G. B. and Khong, P. W. (1993): The effect of varying the support conditions on the buckling of laminated composite plates, *Composite Structures*, 24, 99-106.
19. Chakraborty, S., Mukhopadhyay, M. and Mohanty. A.R. (2000): Free vibrational responses of FRP composite plates: experimental and numerical studies, *Journal of Reinforced Plastics and Composite*, 19, 535-551.
20. Chang, W.P. and Jen, S. (1986): Nonlinear free vibration of heated orthotropic rectangular plates, *International Journal of Solids Structures*, 22 (3), 267-281.
21. Chen, B. and Chou, Tsu-Wei (): Free vibration analysis of orthogonal-woven fabric composites, *Journal of Composites: Part A*, 30, 285-297.
22. Choi, H.S., Ahn, K.J., Nam, J.D. and Chun, H.J. (2001): Hygroscopic aspects of epoxy/carbon fiber composite laminates in aircraft environments, *Composites: Part A*, 32, 709-720.
23. Collings, T.A. and Stone D.E.W. (1985): Hygrothermal effects in CFRP laminates: strains induced by temperature and moisture, Composites, 16(4), 307-316
24. Crawley, E. F. (1979): The Natural Modes of Graphite/Epoxy Cantilever Plates and Shells, *Journal of Composite Materials*, 13, 195-205.
25. Crouzet-Pascal, J. (1978): Buckling analysis of laminated composite plates, *Fibre Science and Technology*, 11, 413-446.
26. Dash, P. and Singh, B. N. (2012): Buckling and post-buckling of laminated composite plates, *Mechanics Research Communications*, 46, 127.

27. Dhanraj, R.D. and Palaninathan (1989): Free vibrational characteristics of composite laminates under initial stress, *Proceedings of the Seminar on Science and Technology of Composite, Adhesives and Sealants*, Bangalore, India, 245-251.
28. Eslami, H. and Maerz, S. (1995): Thermally induced vibration of a symmetric cross-ply plate with hygrothermal effects, *American Institute of Aeronautics of Astronautics Journal*, 33, 1986-1988.
29. Ferreira, A. J. M., Roque, C. N. C. and Jorge, R. M. N. (2005): Free vibration analysis of symmetric laminated composite plates by FSDT and radial basis function, *Computer Methods in Applied Mechanics and Engineering*, 194, 4265-4278.
30. Galea, S.C.P. and White, R.G. (1993): The effect of temperature on the natural frequencies and acoustically induced strains in CFRP plates, *Journal of Sound and Vibration*, 164 (3), 399-424.
31. Gibson R. F. (2007): Principles of composite material mechanics, *CRC Press*.
32. Huang, X., Shen, H. and Zheng, J. (2004): Nonlinear vibration and dynamic response of shear deformable laminated plates in hygrothermal environments, *Composites Science and Technology*, 64, 1419-1435.
33. Hwang, S. and Chang, C. (2000): Determination of elastic constants of materials by vibration testing, *Composite Structures*, 49, 183-190.
34. Iyengar, N.G.R. and Umaretiya, J.R. (1986): Deflection Analysis of Hybrid Laminated Composite Plates, *Composite Structure*, 5, 15-32.
35. Iyengar, N.G.R. and Umaretiya, J.R. (1986): Transeverse vibrations of hybrid laminated plates, *Journal of Sound and Vibration*, 104(3), 425-435.
36. Jones, R.M. (1975): Mechanics of composite materials, *McGraw-Hill*, New York.
37. Ju, F., Lee H.P., and Lee K.H. (1995): Finite Element Analysis of Free Vibration of delaminated Composite plates, *Composite Engineering*, 5, 195-205.
38. Kam, T.Y. and Chang, R.R. (1992): Buckling of shear deformable laminated composite plates, *Composite Structures*, 22, 223-234.
39. Kanematsu, H. H., Hirano, Y. and Hisashi, I. (1988): Bending and Vibration of CFRP-Faced Rectangular Sandwich Plates, *Composite Structures*, 10, 145-163.
40. Lagace, P. A., Jensen, D.W. and Finch, D.C. (1986): Buckling of unsymmetric composite laminates, *Composite Structures*, 5, 101-123.

41. Lei, X., Shujie, W. R. Z. and Yong, L. (2010): Vibration characteristics of glass fibre- epoxy composites with different woven structure, *Journal of Composite Materials*.
42. Lei, X., Shujie, W. R. Z. and Yong, L. (2010): Vibration characteristics of glass fibre- epoxy composites with different woven structure, *Journal of Composite Materials*.
43. Leissa, A.W. (1983): Buckling of composite plates, *Composite Structures*, 1, 51-66.
44. Lin, D.X., Ni R.G. and Adams R.D. (1984): Prediction and Measurement of vibrational damping parameters of Carbon and Glass Fibre-Reinforced Plastic Plates, *Journal of Composite Materials*, 18, 132.
45. Lo, S.H., Zhen, W., Cheung, Y.K. and Wanji, C. (2010): Hygrothermal effects on multilayered composite plates using a refined higher order theory, *Composite Structures*, 92, 633-646.
46. Lopatin, A.V. and Korbut, Y.B. (2006): Buckling of clamped orthotropic plate in shear, *Composite Structures*, 76, 92-98.
47. Maheri, M. R. (2010): The effect of layup and boundary conditions on the modal damping of FRP composite panels, *Journal of Composite Materials*, 45(13) 1411-1422.
48. Maiti, D. K. and Sinha, P. K. (1996): Bending, free vibration and impact response of thick laminated composite plates, *Journal of Computers and Structures*, 59, 115-129.
49. Mania, R. (2005): Buckling analysis of trapezoidal composite sandwich plate subjected to in-plane compression, *Composite Structures*, 69, 482-490.
50. Ovesy, H.R., Ghannadpour, S.A.M. and Zia-Dehkordi, E. (2013): Buckling analysis of moderately thick composite plates and plate structures using an exact finite strip, *Composite Structures*, 95, 697-704.
51. Naik, N.K., Ramasinha, R., Arya, H., Prabhu, S.V. and SharmaRao, N. (2001): Impact response and damage tolerance characteristics of glass-carbon/epoxy hybrid composite plates, *Composites Part B*, 32, 565-574.
52. Ni, R. G., Lin, D. X. and Adams, R. D. (1984): The dynamic properties of carbon-glass fibre sandwich-laminated composites: theoretical, experimental and economic considerations, *Composites*, 15, 297-304.
53. Palady, R.F. and Palazotto A.N. (1990): Buckling and vibration of composite plates using the Levy method, *Composite Structures*, 14, 61-86.

54. Panda, H.S., Sahu, S. K. and Parhi, P.K. (2013): Hygrothermal effects on free vibration of delaminated woven fibre composite plates – Numerical and Experimental results, *Composite Structures*, 96, 502-513.
55. Panda, S. K. and Ramachandra, L. S. (2010): Buckling of rectangular plates with various boundary conditions loaded by non-uniform inplane loads, *International journal of Mechanical Sciences*, 52, 819-828.
56. Parhi, P.K., Bhattacharyya, S.K. and Sinha, P.K. (2001): Hygrothermal effects on the dynamic behaviour of multiple delaminated composite plates and shells, *Journal of Sound and Vibration*, 248(2), 195-214.
57. Patel, B. P., Ganapathi, M. and Makhecha, D. P. (2002): Hygrothermal effects on the structural behaviour of thick composite laminates using higher-order theory, *Composite Structure*, 56, 25-34.
58. Rath, M.K. and Sahu, S.K. (2011): Vibration of woven fiber laminated composite plates in hygrothermal environment, *Journal of Vibration and Control*, 18(3), 1957-1970.
59. Sai Ram, K.S. and Sinha, P.K. (1992): Hygrothermal effects on the free vibration of laminated composite plates, *Journal of Sound and Vibration*, 158(1), 133-148.
60. Sai Ram, K. S. and Sinha, P. K. (1992): Hygrothermal effects on the buckling of laminated composite plates, *Composite Structures*, 21, 233-247.
61. Seifi, R., Khoda-yari, N. and Hosseini, H. (2012): Study of critical buckling loads and modes of cross-ply laminated annular plates, Composites: Part B, 43, 422-430.
62. Singh, G., Sadasiva Rao, Y. V. K. and Iyengar, N. G. R. (1989): Buckling of thick layered composite plates under in-plane moment loading, *Composite Structures*, 13, 35-48.
63. Sundaresan, P., Singh, G. and Rao, G. V. (1996): Buckling and post-buckling analysis of moderately thick laminated rectangular plates, *Computers and Structures*, 61, 79-86.
64. Topal, U. and Uzman, U. (2007): Optimum design of laminated composite plates to maximise buckling load using MFD method, *Thin-Walled Structures*, 45, 660-669.
65. Whitney, J. M. and Ashton, J.E. (1971): Effect of environment on the elastic response of layered composite plates, *American Institute of Aeronautics of Astronautics Journal*, 9, 1708-1713.

66. Xiang, S., Wang, K., Ai, Y., Sha, Y. and Shi, H. (2009): Natural frequencies of generally laminated composite plates using the Gaussian radial basis function and first-order shear deformation theory, *Thin-Walled Structures*, 47, 1265-1271.
67. Xiang, S. and Wang, K. (2009): Free vibration analysis of symmetric laminated composite plates by trigonometric shear deformation theory and inverse multiquadric RBF, *Thin-Walled Structures*, 47, 304-310.
68. Zhong, H. and Gu, C. (2007): Buckling of symmetrical cross-ply composite rectangular plates under a linearly varying in-plane load, *Composite Structures*, 80, 42-48.